Hindawi
Adsorption Science & Technology
Volume 2021, Article ID 6297451, 21 pages
https://doi.org/10.1155/2021/6297451

*Research Article*

# Sequestration of Hazardous Dyes from Aqueous Solution Using Raw and Modified Agricultural Waste

**Mobolaji M. Jegede, Olatunde S. Durowoju, and Joshua N. Edokpayi**

*Faculty of Science, Engineering and Agriculture, University of Venda, Private Bag X5050, Thohoyandou 0950, South Africa*

Correspondence should be addressed to Joshua N. Edokpayi; joshua.edokpayi@univen.ac.za

Received 16 September 2021; Revised 16 November 2021; Accepted 25 November 2021; Published 14 December 2021

Academic Editor: Senthil Kumar Ponnusamy



The continuous degradation of surface water quality by dye materials is of concern globally. Agricultural waste *Litchi chinensis* (LC) peel in its raw (RL) and modified (CL) forms was used as potential sorbents for sequestration of Congo red (CR) dye from an aqueous solution. The sorbents were characterized before and after sorption with Fourier transform infrared spectroscopy (FTIR), scanning electron microscopy (SEM), energy-dispersive X-ray spectroscopy (EDS), Brunauer, Emmett, and Teller (BET) surface area analysis, and X-ray diffraction (XRD). Determination of the point of zero charge (PZC) suggested CR dye sorption from an aqueous solution would be best in acidic pH. Batch experimental drivers such as the effects of time, dosage, initial concentration, pH, and temperature were optimized and used. Results from the study showed that modification with citric acid (CA) reduced the equilibration time from 90 to 15 min. Change in water chemistry did not significantly affect the removal efficiency of the sorbent but rather slightly improved it for both sorbent types. The smaller particle size of <125 $\mu$m recorded higher removal efficiency than the larger one (>125 $\mu$m). The effect of temperature affects the sorption differently. For the RL system, it decreases with an increase in the temperature, while for the CL system it increases with an increase in temperature. The Langmuir isotherm best described the equilibrium data obtained based on the linearized coefficients with maximum sorption capacities ($q_{max}$) of 55.56 mg/g (RL) and 58.48 mg/g (CL). The pseudo-second-order model also best described the kinetic data. The thermodynamics study showed that the reaction is both feasible and spontaneous. Both sorbents recorded high removal efficiency for other dyes such as rhodamine B, methylene blue, methyl orange, malachite green, and erythrosin B. The five cycled regeneration/sorption experiments with 0.1 M NaOH as the desorbing agent showed that the regenerated sorbents efficiently removed CR dye from an aqueous solution close to their virgin samples for the first three cycles. This research, therefore, establishes LC peel as a potential eco-friendly, readily available, and effective sorbent for sequestration of hazardous dyes from wastewater.

## 1. Introduction

Water scarcity and water pollution are major environmental challenges of the 21st century. Clean water is a scarce commodity in most communities of developing countries due to continuous pollution of the limited water resources available by domestic and industrial human activities, a development that may have adverse effect on rural dwellers [1, 2]. Industrial activity is usually accompanied by utilization of large volume of fresh water and generation of large amount of wastewater [3]. Industrial effluent consists of organic and inorganic pollutants such as dyestuff, pesticide residues, solvents and cleaning fluids, dissolved residue from fruit and vegetables, lignin from pulp and paper, brine, and metals [4, 5]. Dyestuff which is one of the major contaminants gets released to the environment through its ever-increasing use by industries such as textile, pulp and paper, leather, tannery, paints, food, pharmaceutical, and electroplating industries [6, 7]. World Bank specifically labelled textile industries as the major consumers of world production of synthetic dyes, also as being responsible for 20% of water pollution globally due to their continuous discharge of coloured wastewater into the environmental media [8].

The discharge of untreated dye effluent into various environment media is a threat on the ecosystem as synthetic dye may be degraded to highly lethal, mutagenic, and carcinogenic products [9, 10]. Human exposure to such water has led to an increase in potential cancer risk, skin irritation, eye inflammation [11], and severe damage to the brain, kidney, liver, reproductive system, and central nervous system [12]. Surface water colouration, which is a resultant effect of dye effluent, reduces aesthetic value of water, thus making it unsuitable for recreation, irrigation, and domestic use. Furthermore, light penetration is significantly reduced thereby hindering photosynthetic activity. This eventually affects growth or brings about death of aquatic lives [10, 13, 14].

There are discharge standards for industrial effluent globally, but unfortunately, the level of compliance is low because existing treatment methods for wastewater are highly expensive and often cause secondary contamination of the environment. Also, these coloured effluents contain mainly azo dyes. This class of dyes is difficult to sequester from wastewater due to their extreme solubility in water and complicated aromatic structure which make them stable and non-biodegradable [15, 16]. Sorption process is considered as a very effective method compared to other available methods of wastewater treatment because it is cost-effective, simply designed, easily operated, and sensitive to targeted contaminant [7, 17, 18]. Commercial activated carbon has been widely used as sorbent for effluent treatment. However, despite its generous use in wastewater treatment, commercial activated carbon remains an expensive material [7, 19, 20]. This has led to the search for low-cost agricultural waste/plant material with similar potential properties to replace commercial activated carbons.

Recent research interests are focusing on the use of various agricultural wastes as sorbent for removal of hazardous dye from industrial effluent. These biowastes are biodegradable and readily available in large amount with little or no value and often cause a disposal problem [10, 21]. Some of the agricultural wastes that have been used in previous studies for sequestration of dyes from aqueous media are corn husk [22], coffee waste [23], banana peel [24], marula seed husk [25], macadamia seed husk [26], and litchi seed [27].

These plant materials sometimes are chemically modified to increase their sorption efficiency, also to reduce the amount of time required for sorption process [28, 29]. Citric acid (CA) has been employed in this study as modifier for *Litchi chinensis* (LC) peels. CA is an example of a nontoxic organic acid that is cheap and naturally abundant in biomass. Structurally, CA contains –OH and –COOH linking groups which are not only effective for loading CA on sorbent but also good chelating groups for removal of pollutants like organic dyes and heavy metals from wastewater [30]. This explains why CA will moderately modify any material without causing secondary pollution [31]. Recent research has reported modification of sorbents with CA for sorption of various dyes [30, 32–35].

CR belongs to the class of azo dyes and is widely used by industries because of its unique effectiveness, but its toxic effect on the environment is of great concern [8, 15]. Findings have shown that it undergoes degradation to form carcinogenic aromatic amines, a product which is highly lethal to the environment and has carcinogenic and mutagenic effect in humans [8]. The aim of this study is to explore the potential of the use of agricultural waste (LC) to sequester hazardous dyes from aqueous solution. Also, we develop a novel sorbent by modifying LC with citric acid. Furthermore, a comprehensive characterization of the sorbents was reported. Various experimental drivers for the sorption of dyes were optimized and employed in this study. The effects of change in water chemistry were also investigated. Various sorption equilibrium and kinetic models were employed to evaluate the sorption traits of the sorbent.

## 2. Materials and Methods

*2.1. Sample Collection, Preparation, and Modification.* LC peels were gathered from litchi fruits purchased at Tshakuma fruit market in Vhembe district, South Africa. The peels were washed several times with distilled water to remove adhering impurities and dried in the oven at constant temperature of 50°C for 3 days. The dried peels (Figure 1) were thereafter grinded using Retsch RS 200 pulveriser. The pulverised litchi peels were sieved with King-test VB 200/300 sieve shaker to obtain fine particulate powder of sizes <125 $\mu$m and >125 $\mu$m. The powdered litchi peels were then stored in airtight containers and termed as raw litchi peel powder (RL).

RL were modified with CA similar to methods described by Yan et al. [34] and Zhang et al. [30]. 10 g of RL was dispensed into 250 mL shaker bottle containing 100 mL of 0.5 M CA. The mixture was agitated at 200 rpm in a water bath shaker at room temperature for 90 min. Thereafter, the slurry was poured into a stainless-steel tray and dried at 50°C in an oven for 24 hours. Afterwards, the temperature of the oven was raised to 120°C for 90 min to allow for thermochemical reaction between the acid and plant material (RL). The dried material was soaked and washed several times with distilled water to remove excess CA. The presence of acid was confirmed by testing the filtrate with 0.1 M lead (ii) nitrate until no turbidity was observed. Lastly, the material was dried in an oven at 50°C for 48 h. The plant material was thereafter allowed to cool, grinded, and sieved again to obtain fine particulate powder of sizes <125 $\mu$m and >125 $\mu$m. These were then stored in an airtight container. This modified plant waste material is termed as CA-modified litchi peel powder (CL).

*2.2. Preparation and Calibration of Dye Solution.* Analytical grade of CR dye was purchased from Fisher Scientific, USA. The structural formula of CR is shown in Figure 2, and its physicochemical properties as presented by Ojo et al. [36] is shown in Table 1. Stock solution of CR dye was prepared by dissolving 1 g of CR dye with deionized water in 1000 mL volumetric flasks. Various test solutions of desired concentrations were prepared by dilution of a known volume of stock solution with appropriate volume of deionized water. The wavelength for maximum CR absorption ($\lambda_{max}$) of 496 nm was predetermined by running a scan on CR solution between 400 and 1000 nm, using a

(a) (b) (c)

Figure 1: Images of (a) litchi peels, (b) pulverised litchi peel (RL), and (c) modified litchi peel (CL).

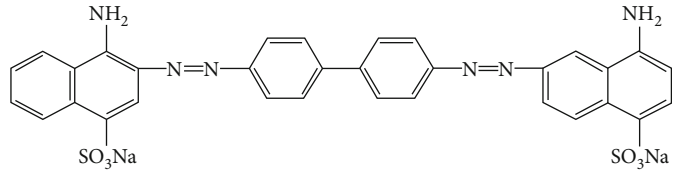


Figure 2: Chemical structure of CR.

Table 1: Physicochemical properties of CR dye.

| | |
|---|---|
| CAS no. | 573-58-0 |
| CA index name | 1-Naphthalenesulfonic acid, 3,30-[(1,10-biphenyl)-4,40-diylbis (2,1-diazenediyl)] bis [4-amino-, sodium salt (1:2)] |
| Molecular formula | $C_{32}H_{22}N_6Na_2O_6S_2$ |
| Molecular weight | 696.66 $gmol^{-1}$ |
| Molecular surface area | 557.6 $Å^2$ |
| Physical form | Brownish-red powder |
| Solubility | Soluble in water, ethanol; very slightly soluble in acetone; practically insoluble in ether, xylene |
| Density | 0.995 $gcm^{-3}$ at 25°C |
| Dye class | Azo |
| Melting point | >360°C |
| pH range | 3.0–5.0 |
| Colour | Blue (pH 3.0) to red (pH 5.0) |
| pKa | 4.1; 3.0 |
| Absorption wavelength ($\lambda_{max}$) | 497 nm; 488 nm |

UV-Vis spectrophotometer (Orion AquaMate 7000, Thermo Scientific).

### 2.3. Characterization of RL and CL

*2.3.1. Fourier Transform Infrared Spectroscopy (FTIR).* The PerkinElmer 100 FTIR spectrophotometer (Waltham, MA, USA) with accessories was utilized to investigate the functional groups responsible for the properties of raw and modified sorbents before and after CR dye sorption. This FTIR spectrophotometer is equipped with Alpha's Platinum ATR (attenuated total reflection) single reflection diamond ATR module with spectral range 7500-375 $cm^{-1}$ and spectral resolution of <2 $cm^{-1}$. The spectroscopy spectra were scanned over the wavelength range of 4000-500 $cm^{-1}$ to capture bands applicable to the sample [37, 38].

*2.3.2. Scanning Electron Microscopy and Energy-Dispersive X-Ray Spectroscopy (SEM-EDS).* Surface morphology and elemental composition of the raw and modified sorbents before and after CR dye sorption were analyzed using a scanning electron microscope (TESCAN, VEGA 3 SBU, Brno, Czech) coupled with an energy-dispersive X-ray spectrometry (EDS) system. This is important in order to understand

the morphology of the surface and to observe any changes in the sorbent brought about by modification and sorption of CR dye. Following the procedure described by Edokpayi et al. [39], powdered sample of sorbents was oven dried at 105°C for 6 h. The samples were sputtered with thin layer of carbon to form a conductive layer around the nonmetallic sample and to prevent accumulation of electron beams. Prior to analysis, the samples were mounted on a metallic stub with a conductive carbon tape. Micrograph of the samples was obtained after irradiation with 20 kV beam of electrons under a vacuum. Analyses of elemental composition of the sorbents were carried out using energy-dispersive X-ray spectroscopy (EDS). Line spectra (peaks) were obtained, each corresponding to an element. The intensity of the characteristic lines is proportionate to the concentration of the element.

*2.3.3. Brunauer, Emmett, and Teller (BET) Technique.* Textural characteristics of powdered sorbents were determined with BET technique using a TriStar II Micromeritics (USA) analyser. Samples were degassed under vacuum at 50°C overnight. Surface area, total pore volume, and average pore diameter were measured using nitrogen gas ($N_2$) at 77 K. Distribution of the pore size and pore volume was determined using the Barrett-Joyner-Halenda (BJH) model [40] and *t*-plot, respectively [41]. Nitrogen molecule cross-sectional area is assumed to be 0.162 $nm^2$. The micropore corresponds to volume sorbed in the pore less than 2 nm, mesopore corresponds to volume sorbed in pores between 2 and 50 nm and, macropore corresponds to volume sorbed in the pore greater than 50 nm.

*2.3.4. X-Ray Diffraction.* PANalytical XPERT-PRO diffractometer (USA) was used for XRD analyses of raw and modified samples of the sorbent before and after CR dye sorption. The samples were grinded into fine particulate powder (<90 $\mu$m) after which they were loaded on the glass sample holder using razor slide to remove any excess and the shutters were closed. Precautions were taken to ensure a tight packing on the glass slit and to avoid manual contamination of the samples [42]. The X-ray diffraction was scanned with the goniometer using the Ni filtered CuK$\alpha$ radiation ($\lambda = 1.5406$ Å) source at an accelerated voltage of 45 kV and a current of 40 mA.

*2.4. Determination of Point of Zero Charge (PZC).* To understand the sorption mechanism, it is necessary to determine the point of zero charge of the sorbent. PZC indicates the pH at which the sorbent is neutral. However, beyond this pH, the sorbent becomes either positively or negatively charged [43]. The PZC of the sorbents were analysed according to the method explained by Ojo *et al.* [36] and Edokpayi et al. [25]. Set up of 7 shaker bottles was made, each containing 40 mL of 0.01 M NaCl. The pH of NaCl solution in each bottle was adjusted to initial pH ($pH_0$) 2, 4, 6, 7, 8, 10, and 12 using 0.1 M HCl and 0.1 M NaOH solutions. The pH of solution was measured using pH meter (Thermo Orion Versa Star). 0.15 g of sorbent was added to each bottle and agitated in water bath shaker at 30°C for 24 hours. After 24 hours, the samples were centrifuged at 2800 rpm for 10 min. The final pH ($pH_f$) of the supernatant was measured. The PZC was estimated by plotting a graph of change in pH ($\Delta pH = pH_0 - pH_f$) against initial pH ($pH_0$). The $pH_{PZC}$ of the sorbent is the point of intersection on the *x*-axis where $pH_f = pH_0$.

*2.4.1. Sorption Study on Effects of Experimental Parameters on the Sorption of CR.* Effect of agitation time was studied from 5 to 180 min to determine the equilibrium time for optimum sorption. Effect of temperature was examined by varying the temperature in the range of 30° to 80°C of each experiment. Different masses of sorbent in the range of 0.02 to 0.20 g were applied on 40 mL of 40, 60, and 80 mg/L concentrations of CR dye solution at optimum time and temperature to investigate the effect of sorbent dose and sorbate concentration. The pH effect was studied to determine the pH condition that favours removal of CR dye from aqueous solution. Seven shaker bottles containing 40 mL of 40 mg/L CR dye solution were set up. The pH of each bottle was adjusted in the range of 2-10 using 0.1 M HCl and 0.1 M NaOH solutions. Sorbent masses in batch of 0.05, 0.10, and 0.15 g were dispensed into each bottle and agitated at optimum time and temperature. Sorbent sizes of <125 $\mu$m and >125 $\mu$m were utilized to investigate the effect of particle size of sorbents on the sorption of CR dye from aqueous solution. All experiments were carried out in triplicate. Consistent trend of the repeat evaluation of sorption parameters observed shows good repeatability of the analyses performed.

*2.4.2. Effect of Matrix.* Water collected from Mutale River (Limpopo province, South Africa) was used to prepare 40 mg/L CR dye solution for batch experiment instead of deionized water used for other experiments. Dye removal efficiencies of experiments conducted using surface water were compared to those of deionized water. This is important to examine the effect of change in water chemistry on the sequestration of CR dye from aqueous solution [25].

*2.5. Removal Efficiency of Other Dyes.* Efficiency of novel sorbents was also tested on the removal of other dyes such as rhodamine B, methylene blue, methylene orange, erythrosin B, and malachite green from aqueous solution. 0.15 g of the sorbent was agitated with 40 mL of 40 mg/L of each dye solution for 180 min. The temperature of the water bath shaker was controlled at 30°C and agitation speed of 200 rpm. Each batch of samples was withdrawn from the shaker at 15 min interval and centrifuged to separate the sorbate from sorbent. Final concentrations of sorbates were determined.

The quantity of dye sorbed $q_e$ (mg/g) was calculated using expression (1), and the removal efficiency of dye sorbed was calculated using expression (2) [38, 44]:

$$q_e = \frac{(C_o - C_e)}{m} \times V, \tag{1}$$

$$\%\text{of dye removal} = \frac{(C_o - C_f)}{C_o} \times 100, \tag{2}$$

where $C_o$ (mg/L) is the initial concentration of the dye solution, $C_e$ (mg/L) is the equilibrium liquid phase concentration of dye, $C_f$ (mg/L) is the final liquid phase concentration of dye, $V$ (L) is the volume of the solution, and $m$ (g) is the mass of the sorbent.

*2.6. Sorption Kinetics.* The mechanism and the rate at which CR dye is sorbed on the surfaces of the sorbents were investigated by applying the Lagergren pseudo-first-order, pseudo-second-order, and intraparticle kinetic models to data generated on sorption study for the effect of time. The linearized expressions for the pseudo-first-order and pseudo-second-order kinetics are presented in equations (3) and (4), respectively [45, 46]:

$$\log\ (q_e - q_t) = \log\ q_e - \left(\frac{k_1 t}{2.303}\right), \tag{3}$$

$$\frac{t}{q_t} = \frac{1}{k_2 {q_e}^2} + \frac{t}{q_e}, \tag{4}$$

where $q_e$ and $q_t$ are the amounts of dye sorbed at equilibrium and at a given time $t$ and $k_1$ and $k_2$ are the rate constants of pseudo-first-order and pseudo-second-order models. The pseudo-first-order kinetic model was used to treat the experimental data obtained by plotting $\log\ (q_e - q_t)$ against time. The values of $k_1$ and $q_e$ were determined from slope and intercept of the plot. Similarly, pseudo-second-order kinetic model was applied to the experimental data by plotting $t/q_t$ against time $t$. The values of $q_e$ and $k_2$ were calculated from the slope and intercept the plot, respectively. The linearity coefficients of the plots obtained were compared in order to determine the best fit kinetic model for the sorption process [39].

Intraparticle diffusion model is linearly expressed as

$$q_t = k_p t^{0.5} + C, \tag{5}$$

where $q_t$ is the amount of dye sorbed (mg/g) at time $t$ (min), $k_p$ is the intraparticle diffusion rate constant (mg/g min), and $C$ is the intercept (mg/L) [47]. This model is further used to treat experimental data obtained by a plot of $q_e$ against $t^{0.5}$. The values of $k_p$ and $C$ can be determined from the slope and intercept of the plot. If the line of the curve passes through the origin and the value of $C = 0$, it is assumed that intraparticle diffusion is the only rate-controlling step of the reaction [48]. The intercept gave an idea about the thickness of the boundary layer. The higher the value of $C$, the greater is the thickness [49]. The calculated value of the slope of the linear plot is the intraparticle rate constant.

*2.7. Sorption Isotherms.* Sorption isotherm describes the performance and interaction of the sorbate with the sorbent [3]. Equilibrium data obtained from the sorption study at different concentrations and temperature were analyzed using Langmuir, Freundlich, and Temkin sorption isotherm models to understand the type of sorption taking place on the surface of the sorbents. The Langmuir model assumes that the sorption of sorbate on an ideal sorbent's surface occurs only at fixed number of sites and each site can only hold one (monolayer) sorbate molecule [50]. It also assumes that all available sites are equivalent and there is no interaction between sorbed molecules on adjacent sites [39]. The linearized expression for the Langmuir model is represented by [51]

$$\frac{1}{q_e} = \frac{1}{q_{\max}} + \left(\frac{1}{K_L q_{\max}}\right)\frac{1}{C_e}, \tag{6}$$

where $C_e$ is the equilibrium concentration of the dye (CR) (mg/L), $q_e$ is the quantity of CR dye sorbed at equilibrium (mg/g), $q_{\max}$ is the maximum amount sorbed (mg/g), and $K_L$ is the Langmuir sorption constant (L/mg). The plot of $1/q_e$ against $1/C_e$ was made, and the values of maximum amount of CR dye sorbed ($q_{\max}$) and the Langmuir sorption constant ($K_L$) were calculated from the intercept and slope of the plot, respectively. The conformity of the sorption process to Langmuir model was determined using

$$R_L = \frac{1}{(1 + K_L C_o)}, \tag{7}$$

where $R_L$ is the separation factor, $C_o$ is the initial dye concentration (mg/L), and $K_L$ is the Langmuir constant (L/mg). $R_L > 1$ indicates unfavourable, $R_L = 1$ indicates linear, $0 < R_L < 1$ indicates favourable, and $R_L = 0$ indicates irreversible monolayer sorption process [39, 52].

The Freundlich isotherm model describes a multisite sorption for heterogeneous surfaces and can be represented by [53]

$$\log q_e = \log K_F + \frac{1}{\mathrm{n}}\ \log C_e \tag{8}$$

where $q_e$ is the quantity of dye sorbed at equilibrium (mg/g), $C_e$ is the equilibrium concentration of dye in solution (mg/L), $K_F$ is the sorption capacity (L/mg), and $1/n$ is the intensity of the sorption showing the heterogeneity of the sorbent site and the energy of distribution [39, 54]. A linear graph of $\log\ q_e$ against $\log\ C_e$ was plotted and the constants $n$ and $K_F$ were determined from the slope and intercept of the plot, respectively. The value of $n > 1$ also indicates favourable sorption process.

Temkin isotherm assumes a linear decrease in the heat of sorption of dye molecules on the sorbent's surface and that this decrease is not logarithmic as stated in Freundlich expression [55]. The linear form of Temkin isotherm is expressed in

$$Q_e = B_1\ \ln\ K_T + B_1\ \ln\ C_e \tag{9}$$

$K_T$ is the equilibrium binding constant ($\mathrm{Lmg}^{-1}$), and $B_1$ is the Temkin constant related to the heat of sorption. Temkin constants $B_1$ and $K_T$ were calculated from the slope an intercept of $q_e$ vs. $\ln\ C_e$.

*2.8. Sorption Thermodynamics.* Thermodynamic study reveals energy changes that occur during sorption process [56]. Data obtained under effect of temperature were employed for thermodynamic study. Spontaneity and

feasibility of the sorption process were determined by thermodynamic parameters such as Gibb's free energy change ($\Delta G^{\circ}$), enthalpy change ($\Delta H^{\circ}$), and entropy change ($\Delta S^{\circ}$). These thermodynamic parameters were calculated based on

$$\ln K_o = \frac{\Delta S^{o}}{R} - \frac{\Delta H^{o}}{RT}, \quad (10)$$

$$\Delta G^{\circ} = -RTlnK_o, \quad (11)$$

where $K_o$ is the equilibrium constant, $R$ is the universal gas constant (8.314 J/mol/K), and $T$ is the temperature (K) [57].

Equilibrium constant $K_o$ has been expressed in literature as $K_o = q_e/C_e$ [32, 44, 52, 58]. However, it is highly important to note that $K_o$ determined through this expression is in the unit of L/g. This must be recalculated as dimensionless to make it fit for thermodynamic equilibrium constant to be used in Van't Hoff plot. It is recalculated by multiplying with molecular weight of sorbate (696.66 g/mol) and concentration of water (55.5 mol/L) [59]. The Van't Hoff plot of ln $K_o$ against $1/T$ should give a linear relationship with the slope of $\Delta H^{\circ}/R$ and an intercept of $\Delta S^{\circ}/R$. Basically, a positive $\Delta H^{\circ}$ value specifies endothermic nature of a sorption process while a negative value implies exothermic reaction. A positive value of $\Delta S^{\circ}$ indicates an increase in randomness at the solid/solution interface that occurs in the sorption process besides reflecting the affinity of the sorbent towards the sorbate. Furthermore, a negative $\Delta G^{\circ}$ value indicates a feasible and spontaneous sorption process at the study temperatures and vice versa.

*2.9. Desorption Study/Regeneration.* Desorption study is highly important especially when considering reusability of the sorbent and safe disposal of spent sorbent into the environment. This brings about practical economics of the wastewater treatment, prevents accumulation of sludge, and alleviates secondary dye contamination of the environment. Desorption experiment was conducted as illustrated by Edokpayi et al. [39]; 0.15 g of the sorbent was dispensed into three 100 mL shaker bottles containing 40 mL of 40 mg/L CR dye solution. These were agitated in an eco-bath shaker controlled at 30°C and agitation speed of 200 rpm for 90 min. After time expiration, the sorbents were recovered and washed with distilled water to remove the residual dye on the surface of the spent sorbent. Deionized water, 0.1 M HCl, and 0.1 M NaOH were utilized as potential desorbing solutions. 40 mL of the desorbing solutions was measured into each 100 mL shaker bottle containing the spent sorbent and agitated for 90 min at a speed of 200 rpm and 30°C. The mixtures were afterward centrifuged, and the supernatant was analysed to determine the final concentration after desorption. The percentage desorption was calculated using expression (12). Regeneration of the sorbents was thereafter investigated by repeating sorption-desorption experiment for 5 cycles to explore the reusability of the sorbents [23].

$$Desorption\% = \frac{\text{Desorbed dye concentration}}{\text{Initial sorbed dye concentration}} \times 100 \quad (12)$$

## 3. Results and Discussion

### 3.1. Characterization of Sorbents

*3.1.1. Fourier Transform Infrared Spectroscopy (FTIR).* The FTIR spectra of RL and CL before and after CR dye sorption are shown in Figure 3. The spectral lines obtained at different band areas indicate that there are various functional groups on the surface of the sorbents. The FTIR spectra of RL and CL as shown in Figure 3(a) show broad band which peaks at 3270 $cm^{-1}$ and represents O-H stretch of the alcohol group [60]. The medium peaks at 2911 and 2841 $cm^{-1}$ represent C-H stretch of the aliphatic group [61]. A strong medium peak at 1603 $cm^{-1}$ characterizes C=C stretch of the aromatic group [56]. Short peaks at 1425 and 1362 $cm^{-1}$ represent the presence of C-H groups. Peaks at 1311 and 1230 ($cm^{-1}$) and sharp peak at 1007 cm-$^{1}$ correspond to C-O stretching [62]. CL spectra show new band at 1491 $cm^{-1}$ assigned to C=O stretching, which implies that carboxyl groups of CA have been introduced to the surface of the sorbent due to modification [30]. Decrease in the intensity of peaks was also observed for CL because the spectra moved to lower absorbance level. This observation reveals the effect of the acid modification at high temperature which brought about intermolecular bond breakage and linkage, thereby capable of enhancing dye sorption [63, 64]. Various functional groups such as hydroxyl, carbonyl, ether, and carboxyl groups available on the surface of the sorbents as revealed by FTIR have been reported to be appropriate for removal of dye [52, 63].

After CR dye sorption, the spectra of spent raw litchi (SRL) reveal a decrease in absorbance values of bands and peaks when compared to RL as presented in Figure 3(b). The reduction of absorbance values suggested that the available sites of the sorbent had been occupied by CR dye. Slight change was observed for CL and its spent form SCL as shown in Figure 3(c). The slight changes indicate that removal of CR dye by RL and CL was more of physisorption than chemisorption. Comparable result was reported by Elavarasan et al. [65].

*3.1.2. Scanning Electron Micrograph (SEM).* The micrographs of both RL and CL before and after sorption of CR dye are shown in Figure 4. The micrographs of RL reveal a faded, free, and less flaky structured surface comparative to that of CL which appeared sharp and more definite, flakier structured surface. The changes observed in the morphology of CL can be attributed to the effect of thermochemical reaction between the modifying agent and plant material, thereby giving it a definite flaky structure. In addition, the surface of CL became sharper and more definite due to removal of impurities such as pectin, lignin, and viscous compounds from the plant material by CA treatment [24, 32]. This observation is relative to the effect of acid modification on the sorbents as reported in the literatures [32, 52].

The SEM micrograph after sorption as shown in images of SRL and SCL reveals more definite and occupied morphology with flaky protuberances which can be attributed to the sorption of CR dye molecule onto the sorbent's active surfaces.

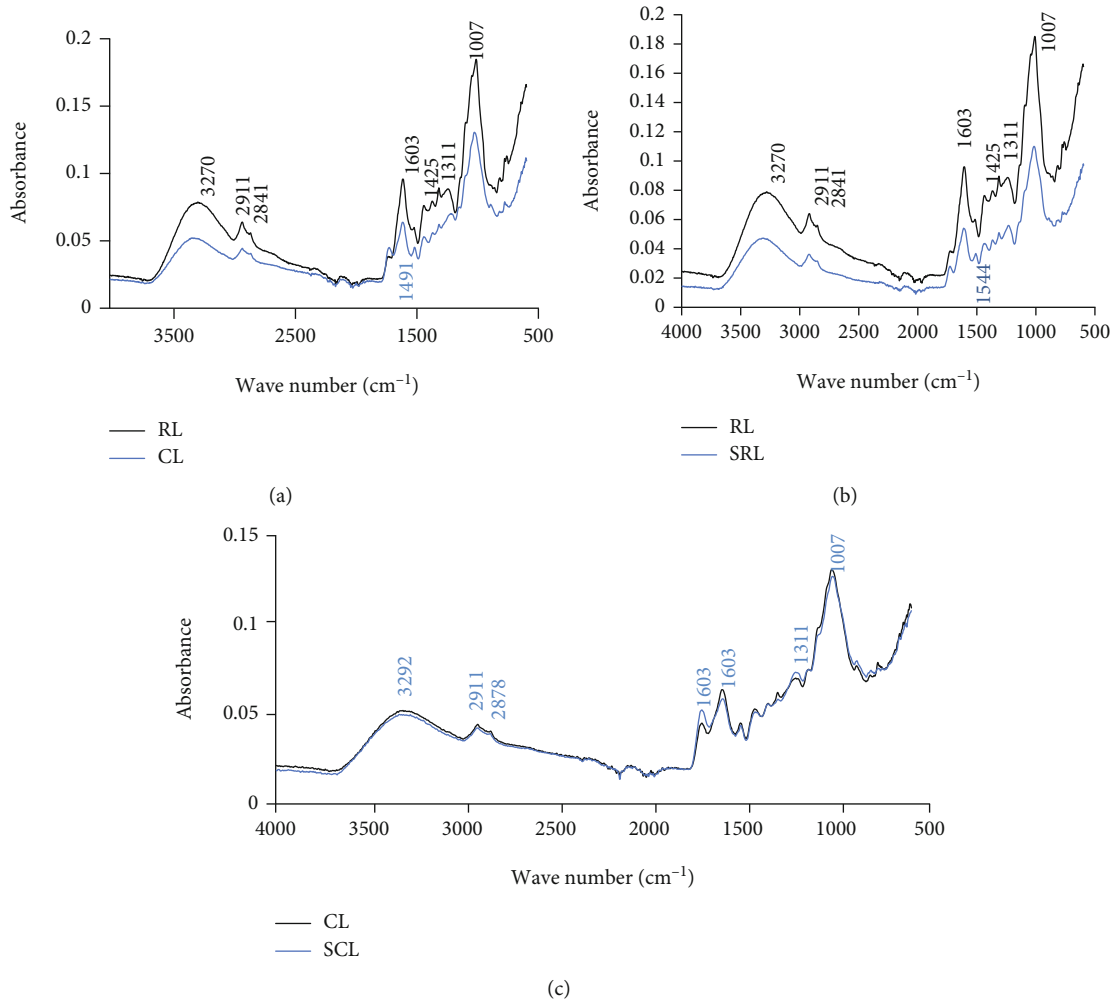


Figure 3: FTIR spectra of (a) RL and CL before sorption, (b) RL and SRL after sorption, and (c) CL and SCL after sorption.

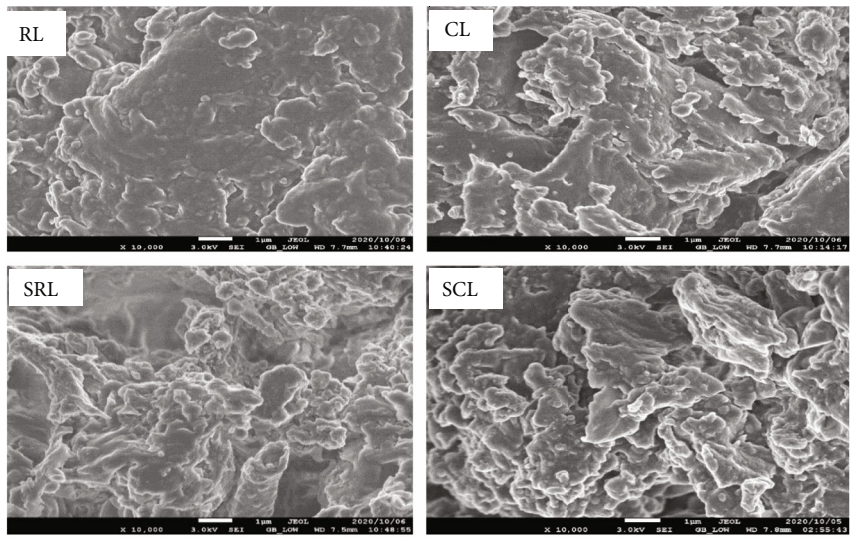


Figure 4: SEM of RL and CL before and after CR dye sorption (×10,000).

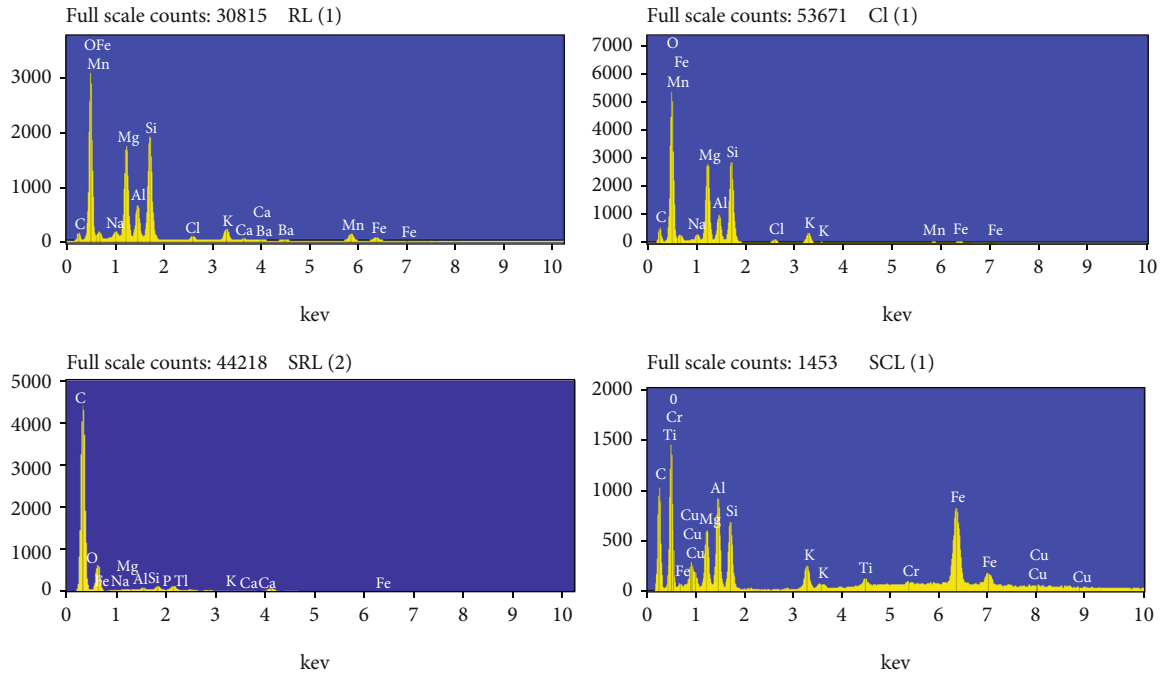


Figure 5: EDX spectra of RL and CL before and after sorption.

*3.1.3. Energy-Dispersive X-Ray Spectroscopy (EDS).* Major elements identified from EDS spectra as shown in Figure 5 were oxygen (O) and carbon (C). Other elements were in minute percentage. The observed increase in atom percentage of carbon and decrease in that of oxygen in the quantitative results of CL compared to that of RL as presented in Table 2 could be due to the thermochemical effect of modification [56]. Modification of sorbents at high temperature destabilised the volatile contents of the sorbent due to bond breakage and linkages thereby resulting in increased percentage of active carbon [36]. As rightfully stated by Bello et al. [66], "the higher the carbon content, the better the sorbent for sorption process." Therefore, CL is capable to have higher dye removal efficiency than RL. After sorption, there is significant increase in atom percentage of carbon and significant reduction in atom percentage of oxygen for the spent sorbents (SRL and SCL). This change thereby confirms that sorption of CR dye onto the sorbents had occured and both RL and CL are suitable sorbent materials for the removal of CR dye from aqueous solution.

*3.1.4. Brunauer, Emmett, and Teller Technique (BET).* Surface area and pore size distribution were analysed by $N_2$ sorption and desorption studies. As presented in Table 3, BET surface area of RL and CL showed low values of 0.4465 $m^2/g$ and 0.6278 $m^2/g$, respectively. The low surface area value is an indication that the sorbents are not microporous in nature; hence, sorption of CR dye may be through the active surfaces, pores, and functional group interaction which is more of physisorption [52]. Some previous research on the sorption of dye from aqueous solution using plant-based sorbents has also reported low surface area values [48, 52, 67]. The observed higher surface area of CL can be credited to acidic washing of the cell wall which eliminated some polar compounds on the surface of the sorbent after modification [52]. After sorption of CR dye, there is reduction in BET surface area values of the spent sorbents due to the sorption of CR dye, which now occupy active surfaces of the sorbents.

Table 2: Elemental composition of RL and CL.

| Biosorbent | Atom % of C | Atom % of O |
|---|---|---|
| RL | 14.40 | 55.91 |
| SRL | 83.06 | 15.52 |
| CL | 24.25 | 54.07 |
| SCL | 59.62 | 18.55 |

Table 3: BET structure parameters of biosorbents before and after dye sorption.

| Biosorbents | BET surface area ($m^2/g$) | Total pore volume ($cm^3/g$) | Average pore diameter (A°) |
|---|---|---|---|
| RL | 0.4465 | -0.000022 | 86.899 |
| SRL | 0.3497 | 0.000273 | 336.486 |
| CL | 0.6278 | 0.000236 | 845.690 |
| SCL | 0.4263 | 0.000186 | 1701.820 |

*3.1.5. X-Ray Diffraction.* The diffraction pattern of a crystalline material shows prominent or sharp peaks while that of an amorphous material shows broad or irregular peaks. The X-ray diffraction plots of RL and CL alongside their respective spent forms (SRL and SCL) after sorption are presented in Figure 6. The diffraction plots of RL and CL displayed broad peaks at 2-thetha angles 13°, 22°, and 43° which are associated with organic functional groups present

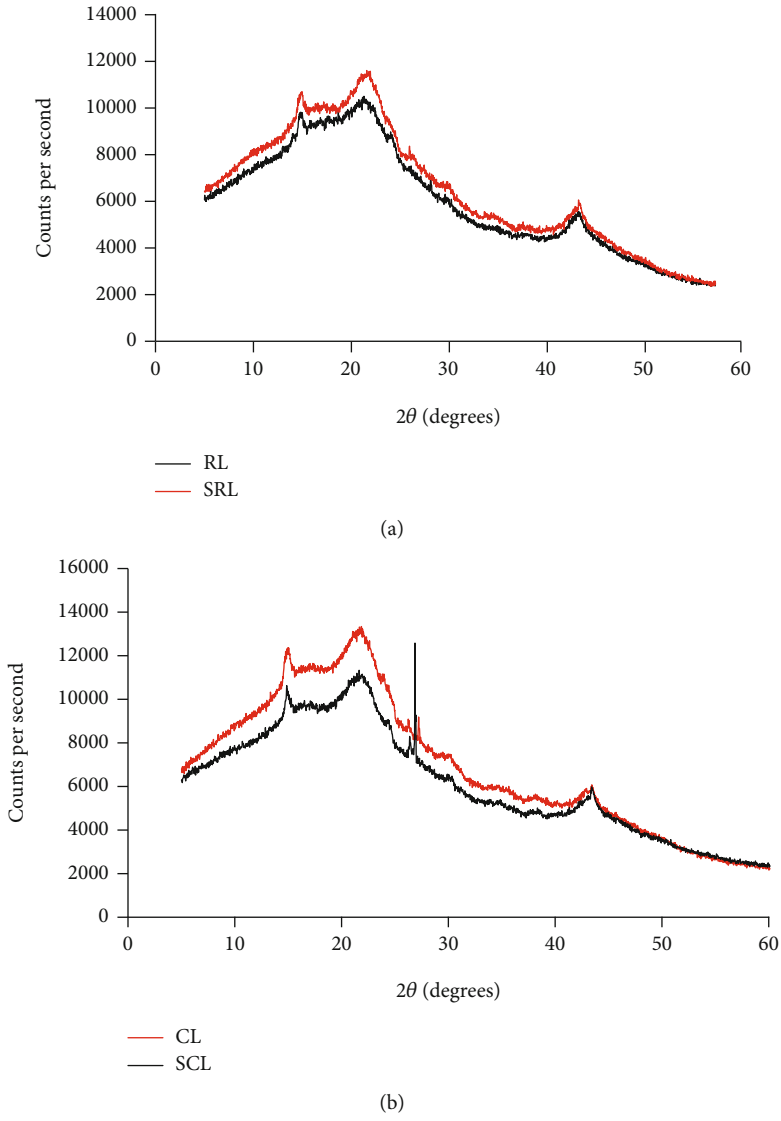


Figure 6: XRD plots of (a) RL and SRL and (b) CL and SCL.

in the sorbents [48]. The diffraction pattern of RL revealed amorphous nature of the sorbent as there were no prominent peaks in the diffraction pattern. CL showed some level of crystallinity due to short sharp peak displayed at 2-theta angle 27° which could be attributed to impact of modification at high temperature. This sharp peak was further intensified/elongated as noticeable in the diffraction pattern of the spent CL (SCL) after sorption of crystalline natured CR dye. This could be attributed to the sorption of CR dye on the upper layer of the sorbent's surfaces [65]. Moreover, diffraction pattern of both spent sorbents (SRL and SCL) moved to higher intensities. This result suggests that dye sorption might induce bulk phase changes of the sorbents.

*3.2. Point of Zero Charge (PZC).* The plots of change in pH against initial pH are shown in Figure 7. $pH_{PZC}$ for RL and CL were determined to be 5.8 and 4.1, respectively. The sorbent's surface is positively charged (attracting anions) when the pH of sorption process is below PZC value. Conversely, above PZC value, the sorbents' surface is negatively charged (attracting cations/repelling anions). The determined PZC for RL and CL are in the acidic region which means that the sorbents would strongly attract anions at acidic pH [68, 69].

### 3.3. Effect of Experimental Parameters on Sorption of CR Dye from Aqueous Solution

*3.3.1. Effect of Contact Time.* The removal efficiency of CR dye by three masses of the sorbents increased rapidly with increasing contact time before attaining equilibrium as shown in Figure 8. It is noteworthy that CL attained equilibrium faster at 15 min than RL with equilibrium time of 90 min. All the masses of the sorbents showed the same level of consistency in attaining equilibrium and beyond equilibrium; there was no further considerable increase in the removal of CR dye. However, RL recorded higher removal efficiency with increasing sorbent dosage while CL removal efficiency is constant irrespective of the increasing dosage.

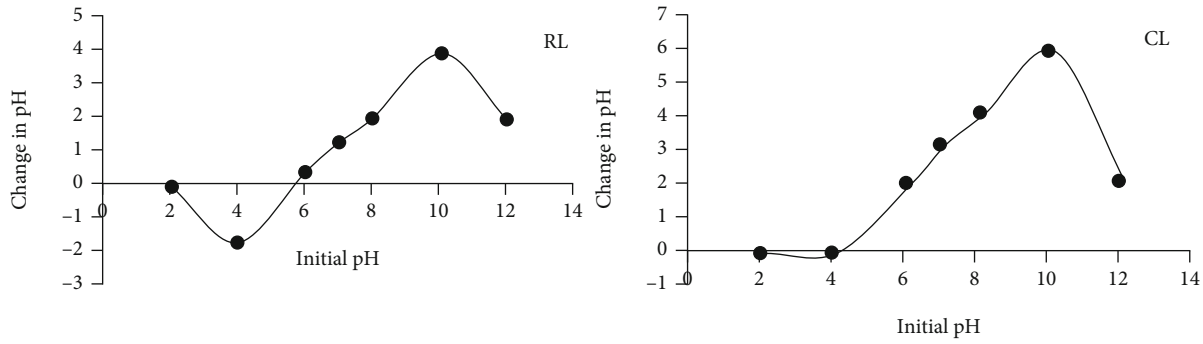


Figure 7: Point of zero charge for RL and CL.

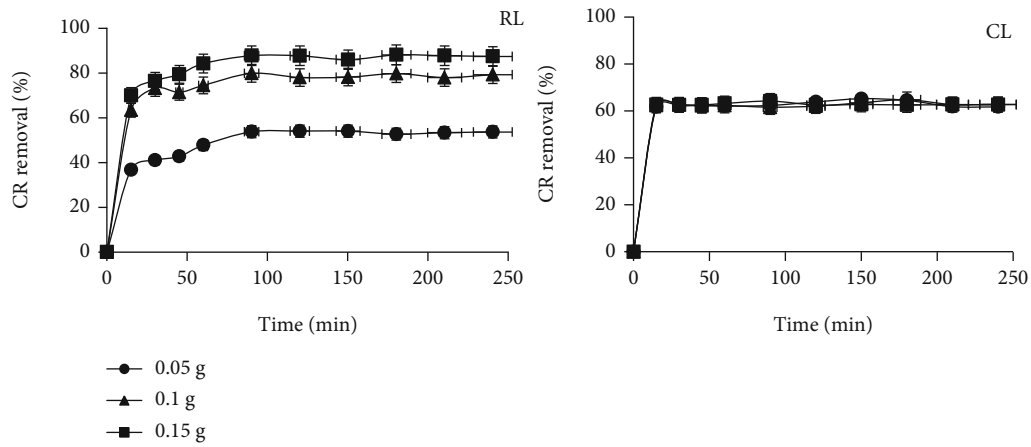


Figure 8: Effect of time on sorption of CR dye onto RL and CL.

This suggests that CL would require less quantity of the sorbent for optimum removal of dye, and optimization of other experimental parameters could help in achieving higher removal efficiency. Faster equilibrium time of CL makes its application more cost-effective than RL. The presence of virgin active sites on the surfaces of the sorbents at the early phase could be responsible for rapid removal efficiency of CR. Stagnation of the sorption efficiency that was observed after equilibrium was attained could be attributed to saturation of the sorbent's surfaces with CR molecules [70, 71]. A similar trend has been observed in some other studies on adsorptive removal of anionic dyes [5, 26, 27, 36]. However, these comparable studies recorded longer equilibrium time.

*3.3.2. Effect of Temperature.* The relationship between the sorption of CR dye from aqueous solution using RL and CL with varying temperature is shown in Figure 9. The results as displayed in the plots show that increase in temperature did not favour sorption of CR dye unto RL, implying an exothermic process. On the contrary, the result for CL shows that increased temperature favoured CR dye removal, indicating an endothermic sorption process. This increase in uptake of CR dye by CL at higher temperature could be credited to increase in mobility of dye molecule and more activation of the sorbent's active sites. This finding agrees with prediction under effect of time that minimal quantity of CL is required for optimum removal of CR dye at high temperature, as the least mass of 0.05 g also achieved high removal efficiency. This means that less sludge is generated for CL system. Study conducted by Olakunle et al. [56] on the sorption of CR by activated cocoa pod husk showed the same trend with increasing temperature, but novel modified sorbent in this study exhibited higher removal efficiency.

*3.3.3. Effect of Dosage and Concentration.* Sorbents' dosage in the range of 0.5 g/L-5.0 g/L was used on different sorbate concentrations of 40, 60, and 80 mg/L, and the plots of the relationship are presented in Figure 10. In general, removal efficiency of CR dye increased with increased sorbent dosage. The lowest concentration of 40 mg/L recorded the highest CR dye removal efficiency compared to other concentrations. It is important to note that RL reached the state of equilibrium at sorbent dosage of 3.5 g/L. However, this state of equilibrium was reached much faster by the modified sorbent CL with lesser dosage of 1.5 g/L. This finding is also consistent with the fact that minimal dosage of CL is required for optimum efficiency; thereby, less sludge is generated. At equilibrium, similar removal efficiencies of CR dye were recorded regardless of the varying sorbent's dosage. The initial increase in the removal efficiency with increased sorbent dosage could be attributed to the corresponding increase in active site available for sorption. The successive supplementary CR removal recorded could result from either aggregation or overlapping of the sorption sites

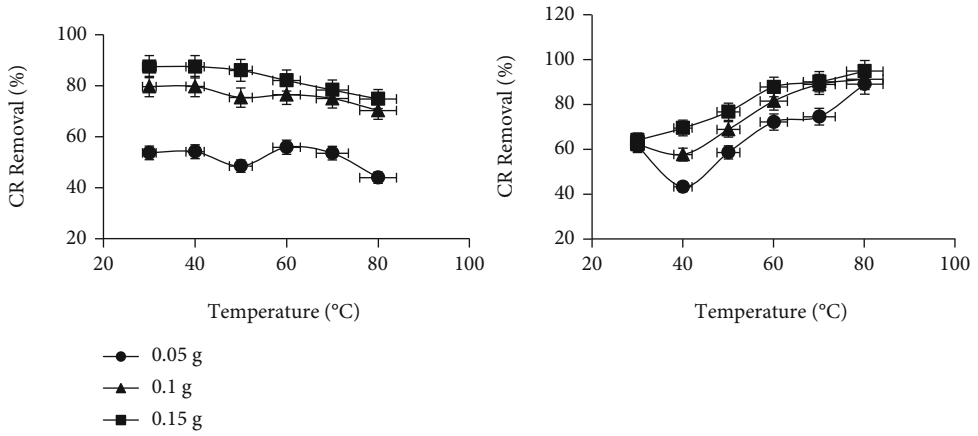


Figure 9: Effect of temperature on sorption of CR dye onto RL and CL.

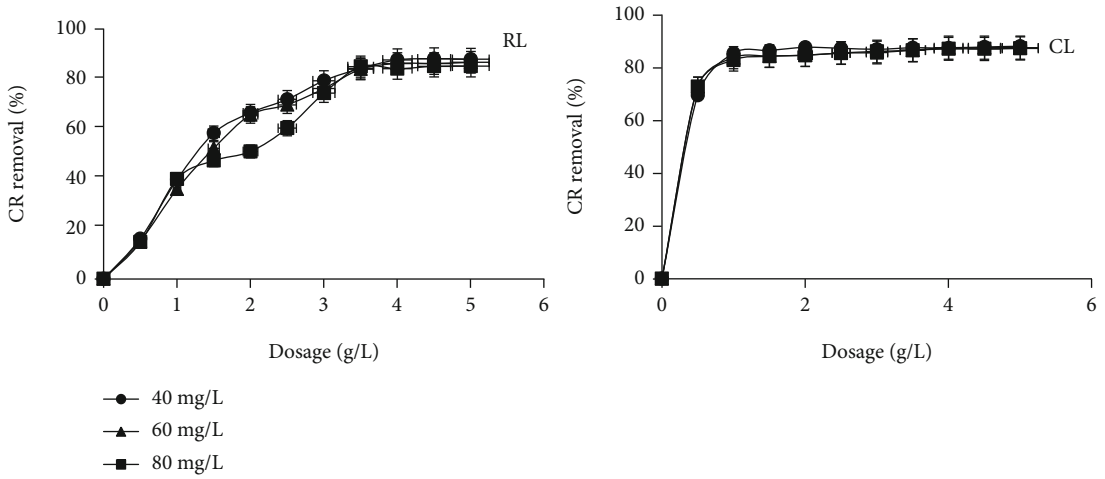


Figure 10: Effect of dosage and concentration on sorption of CR dye onto RL and CL.

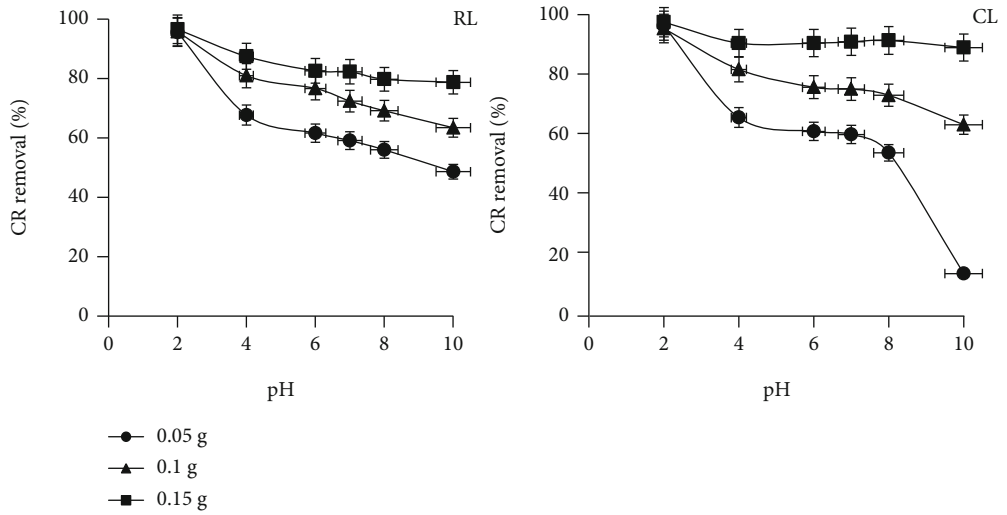


Figure 11: Effect of pH on the uptake of CR dye by RL and CL.

[25]. Due to saturation of sorbent site, very little or no removal was recorded after the state of equilibrium was reached.

*3.3.4. Effect of pH.* The pH of aqueous solution has been established as a significant parameter of a sorption process because of its influence on the surface binding sites of the

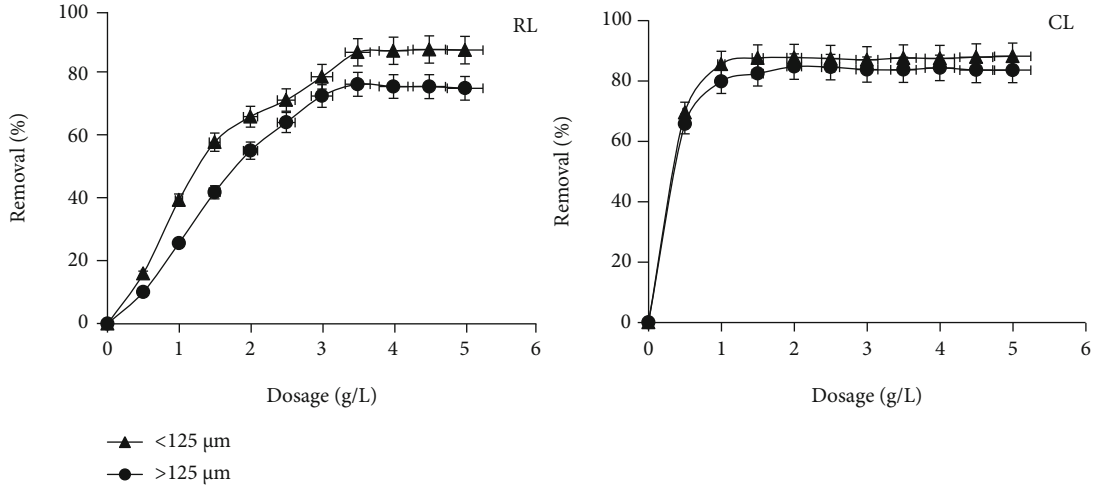


Figure 12: Effect of particle sizes of RL and CL on sorption of CR dye.

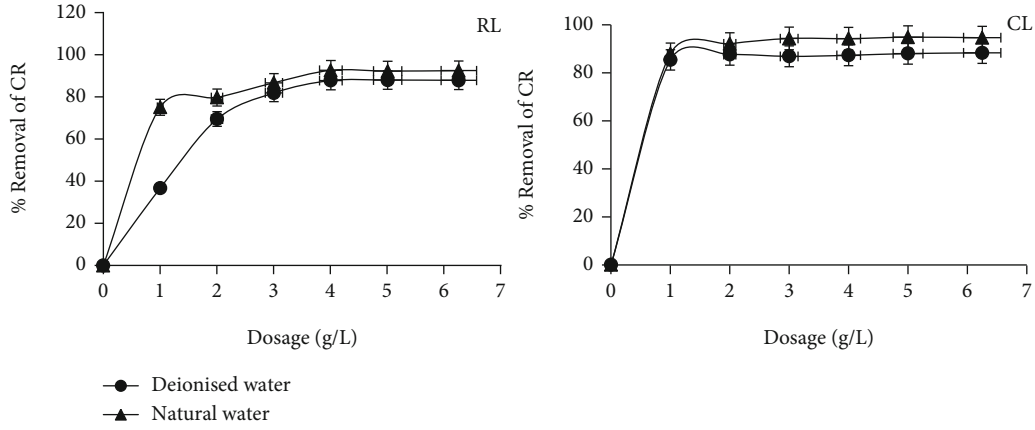


Figure 13: Effect of matrix on sorption of CR dye onto RL and CL.

sorbent and the ionization process of the dye molecule [23, 72]. CR dye is very sensitive to pH change as it turns blue at acidic pH and turns red at basic pH. This colour change in acidic medium is due to protonation, i.e., there is $\pi - \pi^*$ transition of azo group to higher wavelength [23]. The plots of the experimental results as presented in Figure 11 show that maximum CR dye removal percentage was observed at pH 2. Further variation of pH above pH 2 resulted in drastic decline in the removal efficiency of CR dye. This observation agrees with the result obtained for PZC in Section 3.2, which suggested that CR dye removal efficiency would be best in acidic medium.

CR is an anionic dye which dissociates into R-$SO_3^-$ in acidic medium. The maximum sorption of CR dye at pH 2 could be attributed to the existence of strong electrostatic force of attraction between CR in its dissociated state and the positively charged surface of the sorbents [23]. Further increase in pH of the aqueous solution led to increase in negatively charged site and decrease in positively charged site of the sorbents. This brings about electrostatic repulsion between dye anions and negatively charged site of the sorbents, thereby causing a decline in sorption of CR dye [31, 56]. Furthermore, the drastic decrease in sorption of CR at higher pH could also be due to competition for sorption sites between the increased negative ions ($OH^-$) in solution and CR dye molecules [73]. Comparable trends of CR dye sorption using other sorbents had been reported in literature [23, 26, 36, 74].

Table 4: Characteristics of natural water from Mutale River.

| Parameter | Value |
|---|---|
| pH | 6.9 |
| Conductivity ($\mu$S/cm) | 24 |
| Turbidity (NTU) | 14 |
| Sodium (mg/L) | 4.66 |
| Calcium (mg/L) | 2.15 |
| Potassium (mg/L) | 0.35 |
| Magnesium (mg/L) | 1.0 |
| $SO_4^{2-}$ (mg/L) | 3.35 |
| $Cl^-$ (mg/L) | 36.99 |

*3.3.5. Effect of Sorbent Particle Size.* Particle size of a sorbent is an important controlling parameter in the sorption

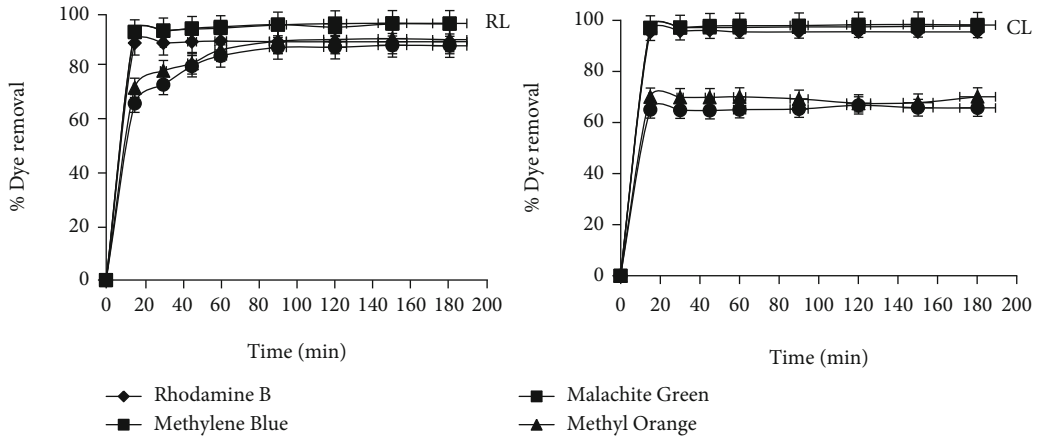


Figure 14: Removal efficiency of RL and CL on selective dyes.

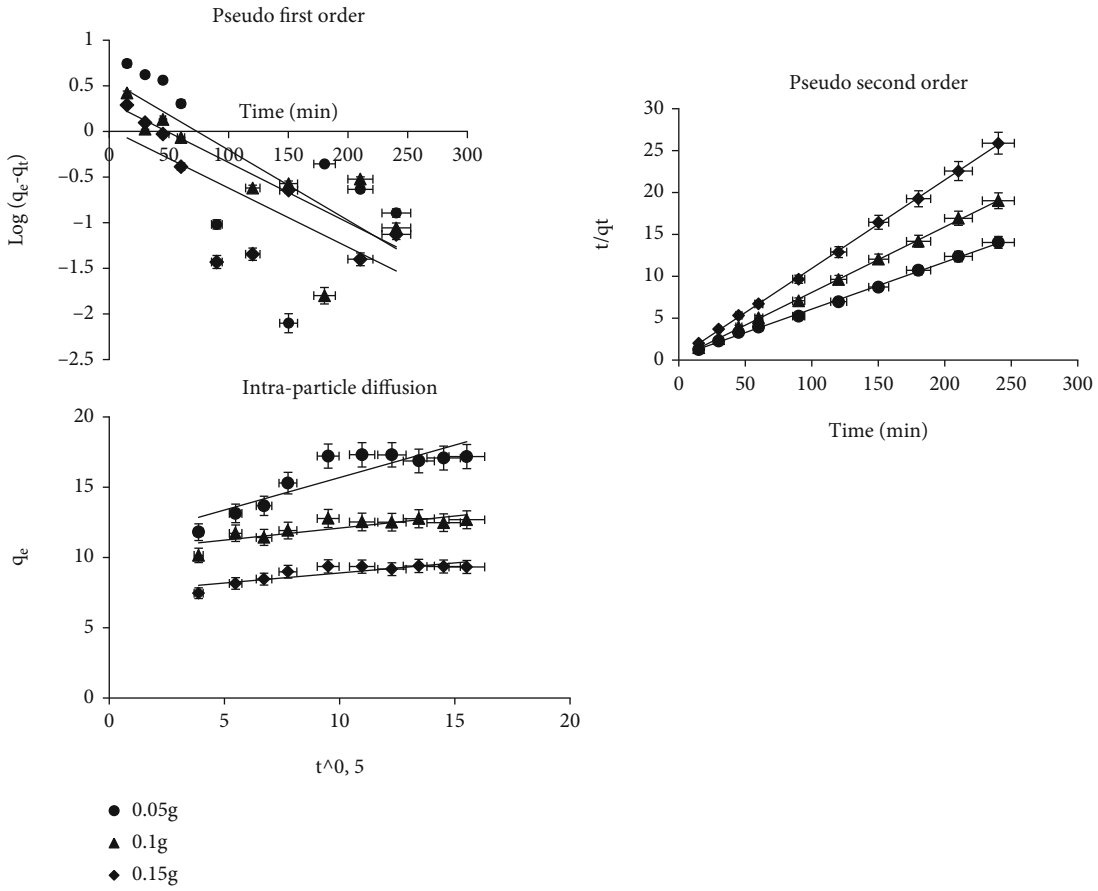


Figure 15: Kinetic model plots of RL.

process because availability of surface area for sorption is greatly influenced by particle size of the sorbent. It can be deduced from the plots shown in Figure 12 that both RL and CL displayed higher CR dye removal efficiencies with particle size of <125 $\mu$m than >125 $\mu$m. This could be attributed to the fact that pulverisation of the sorbents to fine particulate powder provides larger surface area, thereby increasing rate of sorption [75]. This observation is consistent with studies conducted on the sorption of CR dye using biowastes [44, 76].

*3.3.6. Effect of Matrix.* Assessment of experiments conducted with simulated wastewaters prepared from surface water and that of deionized water was made to investigate the influence of change in water chemistry on the sorption of CR dye from aqueous solution. The results as illustrated in Figure 13

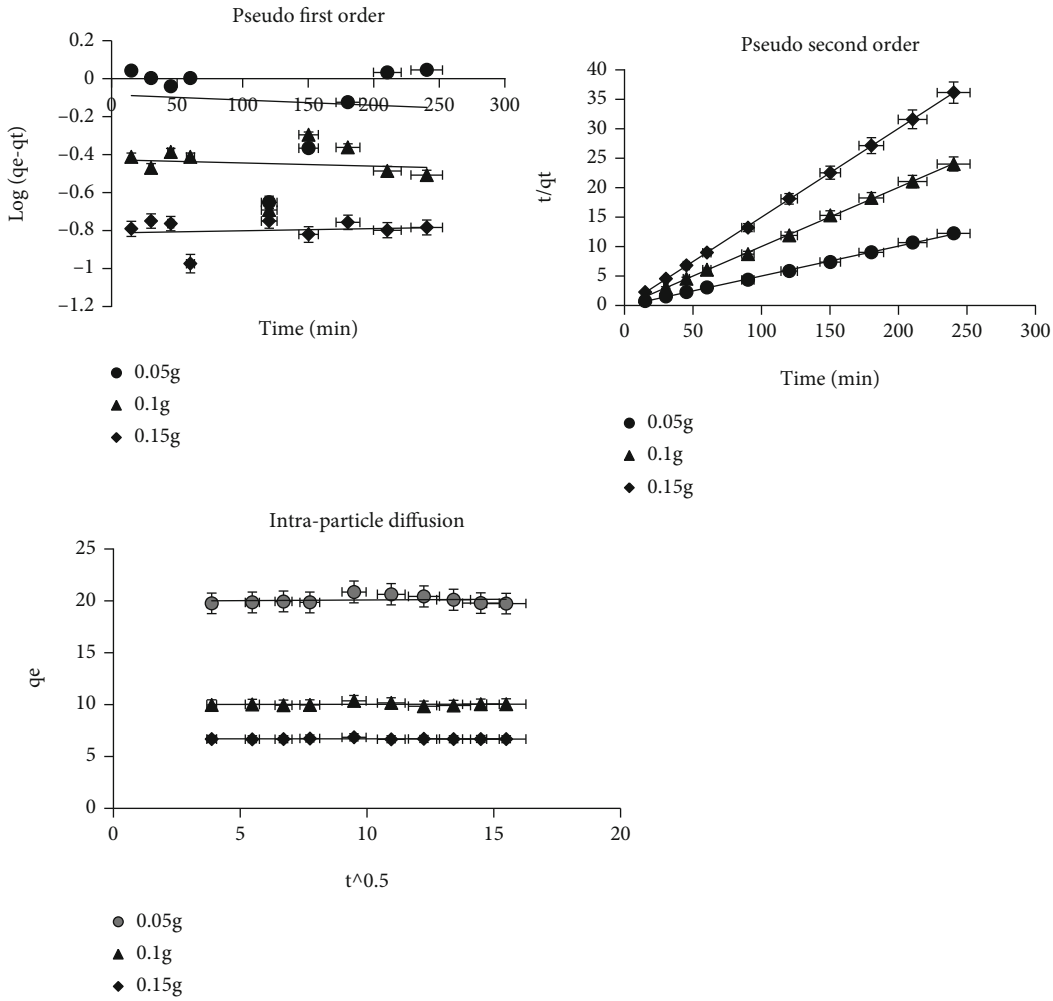


Figure 16: Kinetic model plots of CL.

Table 5: Kinetic model parameters for RL and CL.

| Mass (g) | Pseudo-first-order | | | Pseudo-second-order | | | | Intraparticle diffusion | | |
|---|---|---|---|---|---|---|---|---|---|---|
| | Exp $q_e$ (mg/g) | $K_1$ ($min^{-1}$) | $R^2$ | Exp $q_e$ (mg/g) | Cal $q_e$ (mg/g) | $K_2$ (mg/g $min^{-1}$) | $R^2$ | $K_p$ (mg/g $min^{0.5}$) | $C$ | $R^2$ |
| RL | | | | | | | | | | |
| 0.05 | 3.664 | 0.0180 | 04.575 | 17.168 | 17.889 | 0.0063 | 09.981 | 0.4608 | 11.042 | 07.806 |
| 0.10 | 2.073 | 0.0152 | 06.497 | 12.744 | 12.84 | 0.0213 | 09.995 | 0.1716 | 10.351 | 06.814 |
| 0.15 | 1.062 | 0.0150 | 05.691 | 9.339 | 9.515 | 0.0259 | 09.996 | 0.1427 | 7.457 | 07.348 |
| CL | | | | | | | | | | |
| 0.05 | 0.824 | 0.00069 | 00.094 | 19.704 | 19.802 | 0.0364 | 09.992 | 0.0127 | 19.918 | 00.156 |
| 0.10 | 0.375 | 0.00046 | 00.151 | 9.948 | 9.980 | 0.354 | 09.996 | 0.0007 | 9.998 | 00.004 |
| 0.15 | 6.445 | 0.00023 | 00.189 | 6.667 | 6.658 | 0.388 | 09.999 | -0.0010 | 6.694 | 00.050 |

indicate that higher sorption efficiency of CR dye was achieved in experiment conducted with surface water than that of deionized water. This could be due to catalytic effect of ions present in surface water (Table 4) [25]. These ions tend to speed up uptake of CR dye from the aqueous solution onto the active sites of the sorbents. This trend of higher removal efficiency in natural water agrees with the study conducted by Edokpayi et al. [25], on the influence of change in water chemistry on uptake of methylene blue dye onto macadamia nutshell. This therefore ascertains that sorption process using these sorbents is feasible for sequestration of dye from real wastewater and not just limited to simulated dye solution prepared in the laboratory.

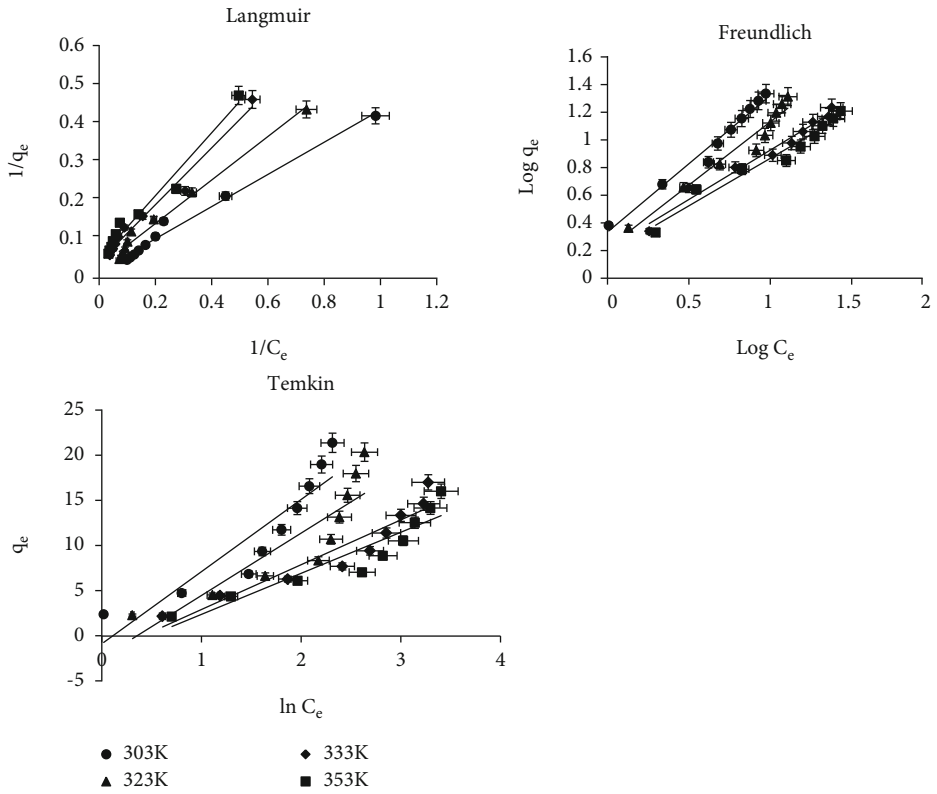


Figure 17: Isotherm model plots of RL.

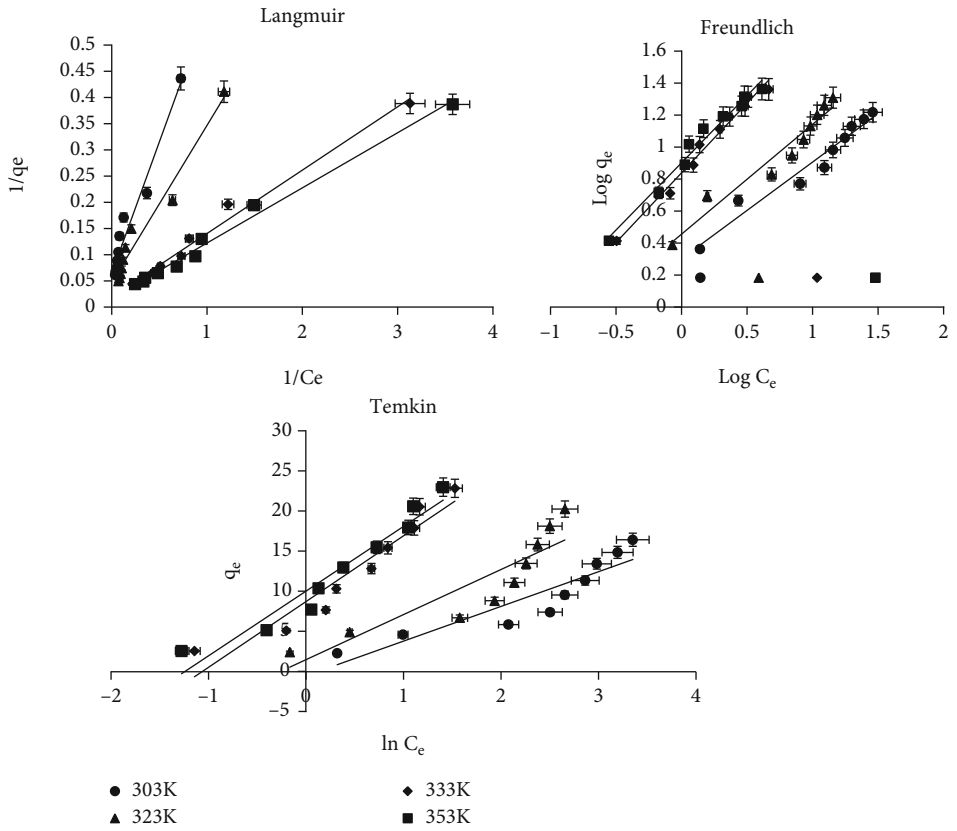


Figure 18: Isotherm model plots of CL.

Table 6: Isotherm model parameters for sorption of CR dye onto RL and CL.

| Temp (K) | Langmuir model | | | Freundlich model | | | Temkin model | | |
|---|---|---|---|---|---|---|---|---|---|
| | $q_{max}$ (mg/g) | $K_L$ (L/mg) | $R^2$ | $R_L$ | $K_F$ (L/mg) | $N$ | $R^2$ | $K_T$ (L/g) | $B$ (J/mol) | $R^2$ |
| RL | | | | | | | | | | |
| 303 | 55.56 | 0.043 | 09.856 | 0.205 | 2.149 | 1.049 | 09.777 | 0.897 | 7.961 | 08.321 |
| 323 | 35.21 | 0.051 | 09.838 | 0.179 | 1.639 | 1.135 | 09.552 | 0.704 | 6.884 | 07.759 |
| 333 | 23.42 | 0.058 | 09.770 | 0.161 | 1.626 | 1.454 | 09.740 | 0.664 | 4.939 | 08.957 |
| 353 | 19.92 | 0.062 | 09.715 | 0.152 | 1.512 | 1.511 | 09.607 | 0.623 | 4.524 | 08.677 |
| CL | | | | | | | | | | |
| 303 | 15.67 | 0.127 | 09.567 | 0.081 | 1.998 | 1.653 | 09.529 | 0.886 | 4.312 | 08.436 |
| 323 | 21.37 | 0.156 | 09.595 | 0.067 | 2.845 | 1.454 | 09.464 | 1.303 | 5.600 | 08.032 |
| 333 | 52.08 | 0.159 | 09.864 | 0.065 | 6.866 | 1.149 | 09.835 | 2.897 | 8.167 | 09.175 |
| 353 | 58.48 | 0.163 | 09.903 | 0.064 | 7.921 | 1.189 | 09.773 | 3.467 | 8.037 | 09.372 |

*3.3.7. Removal Efficiency of Sorbents on Selective Dyes.* Effectiveness of the sorbents on removal of other dyes from aqueous solution was explored, to investigate if the sorbents' potency is not limited to CR (anionic) dye. Five dyes were selected in the group of anionic dyes such as methyl orange and erythrosin B and cationic group such as rhodamine B, methylene blue, and malachite green. The results of the experiment conducted on these selective dyes are presented in Figure 14. It can be deduced from the plots that the sorbents are effective not only for removing CR dye but also effective for the removal of other dyes. In consequence, higher removal percentage was recorded for dyes in the cationic group. This finding confirms the practicability of these novel sorbents for effective sequestration of any other dyes from aqueous solution. CL maintained optimum time (15 min) and mass (0.05 g) for maximum dye removal while RL was at 90 min and 0.15 g, respectively. This makes the modified sorbent advantageous for cost-effective industrial application.

*3.4. Sorption Kinetics.* The linearized plots of kinetic models are presented in Figures 15 and 16, and the results of their parameters are presented in Table 5. From the results obtained, the sorption of CR dye onto the sorbents best fit model is pseudo-second-order model based on its correlation coefficients ($R^2$) values. In addition, the experimental (Exp) and calculated (Cal) values of pseudo-second-order $q_e$ are very close. This shows accuracy of the experiments conducted and further affirms that sorption of CR dye onto RL and CL is pseudo-second-order fitted reactions. Similar outcome has been reported in literature on sorption of CR and other dyes onto various sorbents [5, 23, 26, 30, 31, 56, 76, 77].

In addition, Webber-Morris intraparticle diffusion model was further used to test the sorption data to have understanding about the mechanism and rate controlling steps affecting the sorption kinetics. The fitting of this model consists of various parts that have to do with migration of CR dye from aqueous solution to the surface of the sorbent. These parts are (i) diffusion of CR dye molecules from aqueous solution to the sorbent's surface, i.e., boundary layer diffusion, (ii) transport of CR dye molecules into the intraparticle active sites, i.e., intraparticle diffusion, and (iii) sorption of CR dye molecules to the sorbent's active sites, which is the equilibrium stage [78]. According to the results obtained from the plot of $q_e$ against $t^{0.5}$, the linearity of the plots indicates that intraparticle diffusion is involved in the rate controlling step. However, the fact that the linear plot does not pass through the origin and $C$ value > 0 indicate that intraparticle diffusion is not the only rate-controlling step. This suggests that both surface sorption and intraparticle diffusion are included in the sorption process, therefore a complex sorption mechanism [44].

Table 7: Maximum sorption capacity of CR dye onto various biosorbents in literature.

| Sorbents | Sorption capacity $q_{max}$ (mg/g) | References |
|---|---|---|
| Cashew nutshell | 5.184 | [83] |
| *E. crassipes* roots | 1.580 | [5] |
| Cocoa pod husk (acid activated) | 43.67 | [56] |
| Modified walnut shell | 40 | [36] |
| Pine bark | 3.92 | [79] |
| Cabbage waste powder | 2.313 | [76] |
| Modified coffee waste | 34.36 | [61] |
| Litchi seed powder | 20.49 | [27] |
| Raw litchi peel powder (RL) | 55.56 | This study |
| Modified litchi peel powder (CL) | 58.48 | This study |

*3.5. Sorption Isotherms.* Various linearized plots of isotherm models for raw and modified sorbents are shown in Figures 17 and 18. Isotherm model parameters as presented in Table 6 show that the three models to some extent described the sorption process because they all showed correlation coefficient ($R^2$) values greater than 0.7. However, the sorption data best fit into Langmuir model because it displayed the highest $R^2$ values. This assumes monolayer sorption occurred on a uniform and homogenous sorbent's surface. The conformity of the sorption process to the Langmuir model was further affirmed by a separation factor also known as dimensionless constant ($R_L$). $R_L$ values obtained were between zero and one, which implies favourable

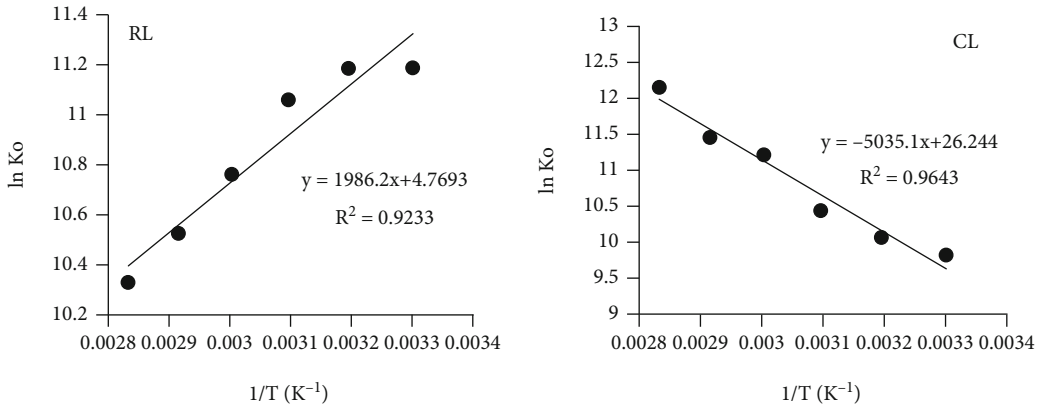


Figure 19: Van't Hoff plots of CR sorption onto RL and CL.

sorption process. In addition, Freundlich model's sorption intensity ($n$) displayed values greater than unity, which is also an indication of favourable sorption process.

Temkin model plots of $q_e$ against ln $C_e$ yielded linear graphs and from the results of the parameters obtained; $K_T$ decreased with increase in temperature for RL and increased with increase in temperature for CL. However, the Temkin model displayed the lowest $R^2$ value of the three models and does not provide best fit for the sorption data.

Comparable studies on the sequestration of CR dye from aqueous solution using various plant-based sorbents also showed conformity to the Langmuir model, and comparison of their maximum sorption capacity ($q_{max}$) to this study is presented in Table 7. It is noteworthy to emphasize that modified sorbent achieved higher sorption capacity than the raw sorbent which could be attributed to significant effect of acid modification. Studies conducted by Yan et al. [34] and Zhang et al. [30] also recorded higher sorption capacity for CA-modified sorbents over raw sorbents.

*3.6. Sorption Thermodynamics.* The Van't Hoff plot of ln $K_o$ against ($1/T$) gives linear graphs for the sorbents as shown in Figure 19, and the values obtained for the parameters are presented in Table 8. With regard to sorption of CR dye from aqueous solution unto RL, negative $\Delta G^\circ$ values were obtained at all working temperatures. This is an indication that the sorption process was spontaneous and feasible. The negative $\Delta H^\circ$ value confirmed that the sorption process was exothermic. The positive value of $\Delta S^\circ$ is an indication that there is increased randomness at the sorbent–sorbate interface during the sorption of CR dye molecules on the active sites. Also, the positive value of $\Delta S^\circ$ infers good attraction of CR dye molecules towards the sorbents. Comparable observations have been reported in literature for sorbents of CR unto other sorbents like coffee waste powder [23] and pine bark powder [79]. Furthermore, the sorption of CR dye unto CL also showed negative values of $\Delta G^\circ$ and positive value for $\Delta S^\circ$. However, the sorption process was endothermic because of the positive $\Delta H^\circ$ value obtained. Comparable observations have also been reported in literature for sorbents of CR onto other sorbents like acid-modified crab shell powder [80] and acid-modified walnut shell powder [36].

Table 8: Thermodynamic parameters for CR dye sorption onto RL and CL.

| Temp (K) | $K_o$ | ln $K_o$ | $\Delta G$ (kJ/mol) | $\Delta H$ (kJ/mol) | $\Delta S$ (J/mol/K) |
|---|---|---|---|---|---|
| RL | | | | | |
| 303 | 72173.98 | 11.18683 | -28.18 | -16.51 | 39.65 |
| 313 | 72042.21 | 11.18501 | -29.11 | | |
| 323 | 63547.37 | 11.05954 | -29.69 | | |
| 333 | 47161.94 | 10.76134 | -29.79 | | |
| 343 | 37247.40 | 10.52534 | -30.02 | | |
| 353 | 30620.63 | 10.32943 | -30.32 | | |
| CL | | | | | |
| 303 | 18349.802 | 9.817374 | -24.73 | 41.86 | 218.19 |
| 313 | 23439.245 | 10.06217 | -26.19 | | |
| 323 | 33893.368 | 10.43097 | -28.01 | | |
| 333 | 73685.913 | 11.20757 | -31.03 | | |
| 343 | 93574.248 | 11.44651 | -32.64 | | |
| 353 | 187969.59 | 12.14404 | -35.64 | | |

*3.7. Probable Sorption Mechanism.* The sorption between the sorbate and sorbent is believed to have occurred via electrostatic interactions and hydrogen bonding between the various functional groups present in the surface of the sorbents and CR. The point of zero charge recorded for the sorbents used in this study is 5.8 (RL) and 4.1 (CL), respectively. This implies that in acidic medium the surface of the sorbents is practically positive and can attract the R–$SO_3^-$ group in the CR molecule via electrostatic interaction. Also, the functional groups recorded from the FTIR spectra of the sorbents such as OH, C=O, and COOH can easily protonate at low pH and attract the negative ions on the sorbate. However, as pH increases, the functional groups in the sorbent surfaces are expected to ionize completely resulting in electrostatic repulsion between CR and the surface of RL and CL which is now negative thus resulting to reduced sorption capacity [23]. Also, the formation of hydrogen bond is more likely as a secondary force of attraction in the sorption process [17]. This is because of the presence of hydrogen and

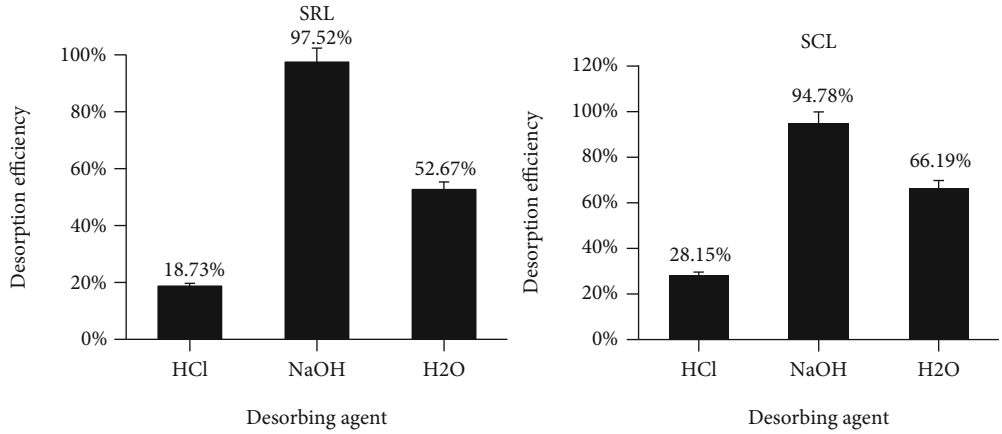


Figure 20: Desorption of SRL and SCL.

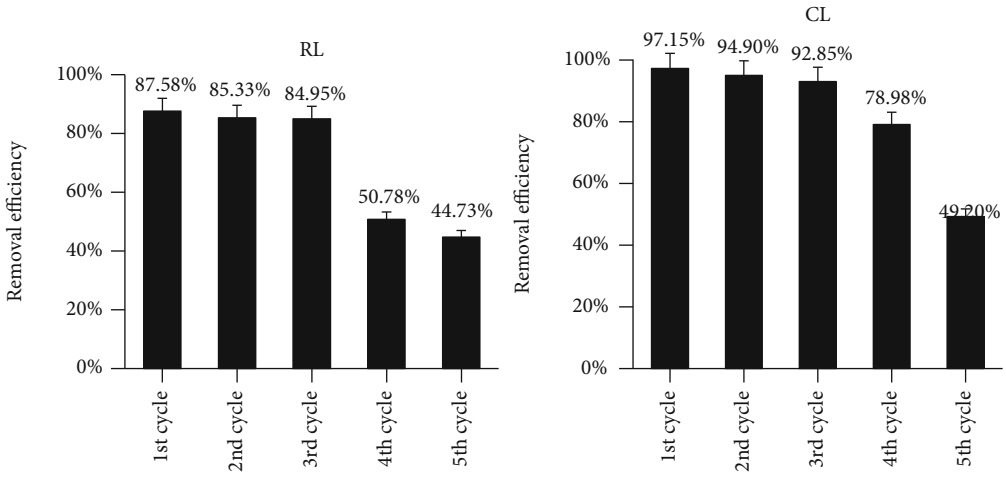


Figure 21: Regeneration and reuse cycles of RL and CL.

highly electronegative atoms such as oxygen and nitrogen on the surface of the sorbent and sorbate.

Previous studies also agree with likelihood of three interactions between the sorbent and dye molecule and which are (i) hydrogen bonding between hydroxyl groups of sorbent and electronegative groups of CR dye, (ii) ionic interactions at pH values where surface charge is neutral and physisorption occurs, and (iii) $\pi$-electron resonance [30, 78].

*3.8. Desorption/Regeneration Study.* The plots of the data obtained from desorption experiment of the spent sorbents are presented in Figure 20. Among the three studied desorbing agents, 0.1 M NaOH most effectively regenerated the spent sorbents as it recorded the highest desorption efficiencies. This suggests that the sorption process is dominated by electrostatic interaction and hydrogen bonding [17, 23]. The solvating strength, concentration of the desorbing agent, and agitation speed all contributed to the migration of CR dye molecules from the solid to liquid phase [81].

Furthermore, regeneration and reuse experiment was thereafter performed by repeated washing of the sorbents with 0.1 M NaOH for five successive cycles. The sorbents were able to sorb CR dye at an amount close to their virgin samples (1st cycle) at the $2^{nd}$ and $3^{rd}$ cycles as shown in Figure 21. However, CL still maintained higher removal efficiency over RL when reused for all cycles. Drastic decline is noticeable in the sorption efficiencies of the $4^{th}$ and $5^{th}$ cycles. The decline could be attributed to difficulty in recovering 100% mass of sorbent in solution and change in superficial structures of sorbents by the alkaline solution [82]. This may subsequently lead to loss and damage/blockage of sorption sites. Similar use of NaOH as effective desorbing agent has been reported in literature by Lafi et al. [23] and Lin et al. [48]. This finding affirms that the novel sorbents can be regenerated and reused; hence, it is a cost-effective technique for the sequestration of hazardous dyes from aqueous solution. The spent sorbent can be safely disposed in a regulated landfill that receives hazardous waste.

## 4. Conclusion

RL and CL were utilized for the sequestration of CR dye from aqueous solution through batch experiment. Characterization of the sorbents revealed the nature, active sites, and functional groups present and elemental composition of the sorbents. Carboxyl group was successfully introduced

to the sorbent's surface by CA modification as revealed by the FTIR spectrum, thus making CL achieve higher sorption capacity with minimal dosage of 1.5 g/L, in 15 min. Sorption process was favoured by acidic pH of 2 and particle size of <125 $\mu$m. Pseudo-second-order kinetic model and Langmuir isotherm model provided the best fit sorption process with $q_{max}$ of 58.48 mg/g for CL and 55.56 mg/g for RL. The sorption process was feasible, spontaneous, and exothermic for RL while that of CL was an endothermic process. Change in water chemistry did not hinder the sorption process. *Litchi chinensis* peel may be considered a potential sorbent for effective sequestration of dyes from wastewater because it was efficient for several dyes.

## Data Availability

The data used in this manuscript is presented in the body of the manuscript.

## Conflicts of Interest

The authors declare no conflict of interest.

## Acknowledgments

The authors are grateful to the funds provided to Dr. JN Edokpayi (Grant number: UID:127276) by the National Research Foundation of South Africa.

## References

[1] J. N. Edokpayi, J. O. Odiyo, and O. S. Durowoju, "Impact of wastewater on surface water quality in developing countries: a case study of South Africa," in *Water Quality Hlanganani Tutu*, pp. 401–416, IntechOpen, 2017.

[2] A. O. Jegede and P. Shikwambane, "Water 'apartheid' and the significance of human rights principles of affirmative action in South Africa," *Water*, vol. 13, no. 8, pp. 1104–1114, 2021.

[3] J. N. Edokpayi, J. O. Odiyo, O. E. Popoola, and T. A. M. Msagati, "Evaluation of contaminants removal by waste stabilization ponds: a case study of Siloam WSPs in Vhembe District, South Africa," *Heliyon*, vol. 7, no. 2, 2021.

[4] R. Malik, D. S. Ramteke, and S. R. Wate, "Adsorption of malachite green on groundnut shell waste based powdered activated carbon," *Waste Management*, vol. 27, no. 9, pp. 1129–1138, 2007.

[5] W. C. Wanyonyi, J. M. Onyari, and P. M. Shiundu, "Adsorption of Congo red dye from aqueous solutions using roots of _Eichhornia crassipes_ : kinetic and equilibrium studies," *Energy Procedia*, vol. 50, pp. 862–869, 2014.

[6] J. N. Edokpayi, S. O. Alayande, A. Adetoro, and J. O. Odiyo, "The equilibrium, kinetics, and thermodynamics studies of the sorption of methylene blue from aqueous solution using pulverized raw macadamia nut shells," *Journal of Analytical Methods in Chemistry*, vol. 2020, 10 pages, 2020.

[7] R. S. Farias, H. L. Buarque, M. B. Cruz, L. M. F. Cardoso, T. A. Gondim, and V. R. Paulo, "Adsorption of Congo red dye from aqueous solution onto amino-functionalized silica gel," *Engenharia sanitária e ambiental*, vol. 23, no. 6, pp. 1053–1060, 2017.

[8] S. Sarkar, A. Banerjee, U. Halder, R. Biswas, and R. Bandopadhyay, "Degradation of synthetic azo dyes of textile industry: a sustainable approach using microbial enzymes," *Water Conservation Science Engineering*, vol. 2, no. 4, pp. 121–131, 2017.

[9] N. Mathur and P. Bhatnagar, "Mutagenicity assessment of textile dyes from Sanganer (Rajasthan)," *Journal of Environmental Biology*, vol. 28, no. 1, pp. 123–126, 2007.

[10] M. A. M. Salleh, P. K. Mahmoud, A. W. A. Karim, and A. Idris, "Cationic and anionic dye adsorption by agricultural solid wastes: a comprehensive review," *Desalination*, vol. 280, no. 1-3, pp. 1–13, 2011.

[11] D. Suteu, B. Doina, and F. Dan, "Synthesis and characterization of polyamide powders for sorption of reactive dyes from aqueous solutions," *Journal of Applied Polymer Science*, vol. 105, no. 4, pp. 1833–1843, 2007.

[12] F. I. Hai, K. Yamamoto, and K. Fukushi, "Hybrid treatment systems for dye wastewater," *Critical Reviews in Environmental Science and Technology*, vol. 37, no. 4, pp. 315–377, 2007.

[13] M. Berradi, R. Hsissou, M. Khudhair et al., "Textile finishing dyes and their impact on aquatic environs," *Heliyon*, vol. 5, no. 11, pp. e02711–e02711, 2019.

[14] N. S. Maurya, A. K. Mittal, and P. Cornel, "Evaluation of adsorption potential of absorbents: a case of uptake of cationic dyes," *Journal of Environmental Biology*, vol. 29, no. 1, pp. 31–36, 2008.

[15] R. D. Saini, "Textile organic dyes: polluting effects and elimination methods from textile wastewater," *International Journal of Chemical Engineering Research*, vol. 9, no. 1, pp. 121–136, 2017.

[16] C. Zaharia and D. Suteu, "Optimization study of Orange 16 dye sorption onto sawdust wastes," *Chemistry and Chemical Engineering, Tom LV (LIX), f.*, vol. 4, pp. 103–113, 2009.

[17] R. Ahmad and R. Kumar, "Adsorptive removal of Congo red dye from aqueous solution using bael shell carbon," *Applied Surface Science*, vol. 257, no. 5, pp. 1628–1633, 2010.

[18] Y. F. Feng, F. Yang, Y. Q. Wang et al., "Basic dye adsorption onto an agro-based waste material - sesame hull (_Sesamum indicum_ L.)," *Bioresource Technology*, vol. 102, no. 22, pp. 10280–10285, 2011.

[19] S. T. Akar, A. S. Özcan, T. Akar, A. Özcan, and Z. Kaynak, "Biosorption of a reactive textile dye from aqueous solutions utilizing an agro-waste," *Desalination*, vol. 249, no. 2, pp. 757–761, 2009.

[20] Y. C. Sharma and S. N. U. Uma, "An economically viable removal of methylene blue by adsorption on activated carbon prepared from rice husk," *Canadian Journal of Chemical Engineering*, vol. 89, no. 2, pp. 377–383, 2011.

[21] K. S. Tushar and S. Dawood, "Review on dye removal from its aqueous solution into alternative cost effective and nonconventional adsorbents," *Journal of Chemical and Process Engineering*, vol. 1, no. 104, pp. 1–7, 2014.

[22] D. S. Malik, C. K. Jain, K. Y. Anuj, K. Richa, and V. P. Vinayak, "Removal of methylene blue dye in aqueous solution by agricultural waste," *International Research Journal of Engineering and Technology*, vol. 3, no. 7, pp. 864–880, 2016.

[23] R. Lafi, I. Montasser, and A. Hafiane, "Adsorption of Congo red dye from aqueous solutions by prepared activated carbon with oxygen-containing functional groups and its regeneration," *Adsorption Science & Technology*, vol. 37, no. 1-2, pp. 160–181, 2019.

[24] A. A. Oyekanmi, A. Ahmad, K. Hossain, and M. Rafatullah, "Adsorption of rhodamine B dye from aqueous solution onto acid treated banana peel: response surface methodology, kinetics and isotherm studies," *PLoS One*, vol. 14, no. 5, pp. 1–20, 2019.

[25] J. N. Edokpayi, S. S. Ndlovu, and O. J. Odiyo, "Characterization of pulverized Marula seed husk and its potential for the sequestration of methylene blue from aqueous solution," *BMC Chemistry*, vol. 13, no. 1, pp. 1–14, 2019.

[26] M. M. Felista, W. C. Wanyonyi, and G. Ongera, "Adsorption of anionic dye (reactive black 5) using macadamia seed husks: kinetics and equilibrium studies," *Scientific African*, vol. 7, 2020.

[27] J. N. Edokpayi and E. Makete, "Removal of Congo red dye from aqueous media using litchi seeds powder: equilibrium, kinetics and thermodynamics," *Physics and Chemistry of the Earth*, vol. 123, no. 7, 2021.

[28] M. Anbia and S. Amirmahmoodi, "Removal of Hg (II) and Mn (II) from aqueous solution using nanoporous carbon impregnated with surfactants," *Arabian Journal of Chemistry*, vol. 9, pp. S319–S325, 2016.

[29] J. Wang, M. Rafatullah, M. Norhashimah, H. Kaizar, and T. T. Teng, "Extraction of toxic rhodamine B dye by using organic solvent: a statistical analysis," *Research Journal of Environmental Toxicology*, vol. 10, pp. 152–158, 2016.

[30] H. Zhang, J. Zhou, Y. Muhammad et al., "Citric acid modified bentonite for Congo red adsorption," *Frontiers in Materials*, vol. 6, no. 5, pp. 1–11, 2019.

[31] Y. Zhou, L. Ge, and N. Fan, "Adsorption of Congo red from aqueous solution onto shrimp shell powder," *Adsorption Science & Technology*, vol. 36, no. 5-6, pp. 1310–1330, 2018.

[32] Y. Ren, C. Cui, and P. Wang, "Pomelo peel modified with citrate as a sustainable adsorbent for removal of methylene blue from aqueous solution," *Molecules*, vol. 23, no. 6, p. 1342, 2018.

[33] Y. Y. Wang, H. Z. Shi, H. B. Zhang, S. M. Yu, N. H. Chen, and Z. F. Tong, "Research on Cr (VI) adsorption with magnetic citric acid bentonite," *Journal of Chemical Engineering of Chinese Universities*, vol. 3, pp. 726–732, 2017.

[34] J. Yan, G. Lan, H. Qiu, C. Chen, Y. Liu, and G. Du, "Adsorption of heavy metals and methylene blue from aqueous solution with citric acid modified peach stone," *Separation Science and Technology*, vol. 53, no. 11, pp. 1678–1688, 2018.

[35] J. B. Zhao, Z. D. Zou, R. Ren, X. F. Sui, Z. P. Mao, and H. Xu, "Chitosan adsorbent reinforced with citric acid modified $\beta$-cyclodextrin for highly efficient removal of dyes from reactive dyeing effluents," *European Polymer Journal*, vol. 108, pp. 212–218, 2018.

[36] T. A. Ojo, A. T. Ojedokun, and O. S. Bello, "Functionalization of powdered walnut shell with orthophosphoric acid for Congo red dye removal," *Particulate Science and Technology*, vol. 37, no. 1, pp. 74–85, 2017.

[37] J. N. Edokpayi, A. M. Enitan-Folami, A. O. Adeeyo, O. S. Durowoju, A. O. Jegede, and J. O. Odiyo, "Recent trends and national policies for water provision and wastewater treatment in South Africa," in *Water Conservation and Wastewater Treatment in BRICS Nations*, pp. 187–211, Elsevier, 2020.

[38] T. O. Ologundudu, J. O. Odiyo, and G. E. Ekosse, "Fluoride sorption efficiency of vermiculite functionalised with cationic surfactant: isotherm and kinetics," *Applied Sciences*, vol. 6, no. 10, p. 277, 2016.

[39] J. N. Edokpayi, J. O. Odiyo, T. A. M. Msagati, and E. O. Popoola, "A novel approach for the removal of lead (II) ion from wastewater using mucilaginous leaves of Diceriocaryum eriocarpum plant," *Sustainability*, vol. 7, no. 10, pp. 14026–14041, 2015.

[40] E. P. Barrett, L. G. Joyner, and P. P. Halenda, "The determination of pore volume and area distributions in porous substances. I. Computations from nitrogen isotherms," *Journal of the American Chemical Society*, vol. 73, no. 1, pp. 373–380, 1951.

[41] B. C. Lippens, B. G. Linsen, and J. H. De Boer, "Studies on pore systems in catalysts I. The adsorption of nitrogen; apparatus and calculation," *Journal of Catalysis*, vol. 4, no. 3, pp. 319–323, 1965.

[42] F. D. S. Marquis, *Proceedings of the 8th pacific rim international conference on advanced materials and proceeding (Pricm-8)*, Springer, Waikoloa, Hawaii, 2013.

[43] A. Achmad, J. Kassim, T. K. Suan, R. C. Amat, and T. L. Seey, "Equilibrium, kinetic and thermodynamic studies on the adsorption of a direct dye onto a novel green adsorbent developed from Uncaria gambir extract," *Journal of Physical Science*, vol. 23, no. 1, pp. 1–13, 2012.

[44] R. Singh, T. S. Singh, J. O. Odiyo, J. A. Smith, and J. N. Edokpayi, "Evaluation of methylene blue sorption onto low-cost biosorbents: equilibrium, kinetics, and thermodynamics," *Journal of Chemistry*, vol. 2020, 11 pages, 2020.

[45] Y. S. Ho and G. McKay, "Kinetic model for lead (II) sorption on to peat," *Adsorption Science & Technology*, vol. 16, no. 4, pp. 243–255, 1998.

[46] S. K. Lagergren, "About the theory of so-called adsorption of soluble substances," *Kung Svenska Veenskapsakad Handingari*, vol. 24, pp. 1–39, 1898.

[47] W. J. Weber and J. C. Morris, "Kinetics of adsorption on carbon from solution," *Journal of Sanitary Engineering Division ASCE*, vol. 89, no. 2, pp. 31–59, 1963.

[48] D. Lin, F. Wu, Y. Hu et al., "Adsorption of dye by waste black tea powder: parameters, kinetic, equilibrium, and thermodynamic studies," *Journal of Chemistry*, vol. 2020, Article ID 5431046, 13 pages, 2020.

[49] N. C. Corda and M. S. Kini, "A review on adsorption of cationic dyes using activated carbon," *MATEC Web of Conferences*, vol. 144, 2018.

[50] I. W. Mwangi, J. C. Ngila, and J. O. Okonkwo, "A comparative study of modified and unmodified maize tassels for removal of selected trace metals in contaminated water," *Toxicological & Environmental Chemistry*, vol. 94, no. 1, pp. 20–39, 2012.

[51] I. Langmuir, "The constitution and fundamental properties of solids and liquids. Part I. Solids," *Journal of American Chemical Society*, vol. 38, no. 11, pp. 2221–2295, 1916.

[52] A. A. Inyinbor, F. A. Adekola, and G. A. Olatunji, "Adsorption of rhodamine B dye from aqueous solution on Irvingia gabonensis biomass: kinetics and thermodynamics studies," *South African Journal of Chemistry*, vol. 68, pp. 115–125, 2015.

[53] H. M. F. Freundlich, "Over the adsorption in solution," *Zeitschriftfur Physikalische Chemie (Leipzig)*, vol. 57, pp. 385–470, 1906.

[54] O. F. Olorundare, T. A. M. Msagati, R. W. M. Krause, J. O. Okonkwo, and B. B. Mamba, "Steam activation, characterisation and adsorption studies of activated carbon from maize tassels," *Chemistry and Ecology*, vol. 30, no. 5, pp. 473–490, 2014.

[55] M. Temkin and V. Pyzhev, "Kinetics of ammonia synthesis on promoted iron catalysts," *Acta Physiochimica. URSS*, vol. 12, no. 3, pp. 217–222, 1940.

[56] M. O. Olakunle, A. A. Inyinbor, A. O. Dada, and O. S. Bello, "Combating dye pollution using cocoa pod husks: a sustainable approach," *International Journal of Sustainable Engineering*, vol. 11, no. 1, pp. 4–15, 2017.

[57] J. H. Van't Hoff, *Studies in dynamic chemistry*, 1884, https://www.nobelprize.org/prizes/chemistry/1901/hoff/biographical/.

[58] N. Javid, Z. Honarmandrad, and M. Malakootian, "Ciprofloxacin removal from aqueous solutions by ozonation with calcium peroxide," *Desalination and Water Treatment*, vol. 174, pp. 178–185, 2020.

[59] X. Zhou and X. Zhou, "The unit problem in the thermodynamic calculation of adsorption using the Langmuir equation," *Chemical Engineering Communications*, vol. 201, no. 11, pp. 1459–1467, 2014.

[60] C. J. Duran-Valle, "Techniques employed in the physicochemical characterization of activated carbons," in *Lignocellulosic Precursors Used in the Synthesis of Activated Carbon-Characterization Techniques and Applications in the Wastewater Treatment*, pp. 37–55, Intech Publisher, Croatia, 2012.

[61] S. Wong, N. Abd Ghafar, N. Ngadi et al., "Effective removal of anionic textile dyes using adsorbent synthesized from coffee waste," *Scientific Reports*, vol. 10, no. 1, pp. 1–10, 2020.

[62] J. Coates, "Interpretation of infrared spectra, a practical approach," in *Encyclopedia of Analytical Chemistry*, R. A. Meyers, Ed., pp. 10815–10837, John Wiley & Sons Ltd, Chichester, 2000.

[63] O. S. Bello and M. A. Ahmad, "Adsorptive removal of synthetic dye using cocoa pod husks," *Toxicological and Environmental Chemistry*, vol. 93, no. 7, pp. 1298–1308, 2012.

[64] S. Kaur, S. Rani, and R. K. Mahajan, "Adsorption kinetics for the removal of hazardous dye Congo red by biowaste materials as adsorbents," *Journal of Chemistry*, vol. 2013, Article ID 628582, 12 pages, 2013.

[65] A. Elavarasan, S. Chitradevi, V. Nandhakumar, S. Sivajiganesan, and S. Kadhiravan, "FT-IR spectra, XRD and EDX studies on the adsorption of methylene blue dye present in aqueous solution onto acid activated carbon prepared from Mimusops elengi leaves," *Journal of Applied Chemistry*, vol. 11, no. 7, p. 51, 2018.

[66] O. S. Bello, M. Auta, and O. B. Ayodele, "Ackee apple (Blighia sapida) seeds: a novel adsorbent for the removal of Congo red dye from aqueous solutions," *Chemistry and Ecology*, vol. 29, no. 1, pp. 58–71, 2013.

[67] S. Sharma and D. P. Tiwari, "Model-fitting approach for methylene blue dye adsorption onCamelinaandSapindusseeds-derived adsorbents," *Adsorption Science & Technology*, vol. 34, no. 9-10, pp. 565–580, 2016.

[68] O. S. Bello, E. O. Alabi, K. A. Adegoke, S. A. Adegboyega, A. A. Inyinbor, and A. O. Dada, "Rhodamine B dye sequestration using Gmelina aborea leaf powder," *Heliyon*, vol. 5, pp. 1–13, 2020.

[69] T. Santhi, S. Manonmani, V. S. Vasantha, and Y. T. Chang, "A new alternative adsorbent for the removal of cationic dyes from aqueous solution," *Arabian Journal of Chemistry*, vol. 9, no. 1, pp. S466–S474, 2016.

[70] T. Tarmizi, M. Risfidian, D. Rohendi, and A. Lesbani, "Kinetic and thermodynamic adsorption studies of Congo red on bentonite," *AIP Conference Proceedings, Yogyakarta: AIP Publishing*, vol. 1823, pp. 020028-1–020028-8, 2017.

[71] M. K. Toor, "Enhancing adsorption capacity of Bentonite for dye removal: physiochemical modification and characterization in Department of Chemical Engineering," University of Adelaide, 2010.

[72] R. Jain and S. Sikarwar, "Adsorption and desorption studies of Congo red using low-cost adsorbent: activated de-oiled mustard," *Desalination and Water Treatment*, vol. 52, no. 37-39, pp. 7400–7411, 2014.

[73] L. Q. Ge, Y. Z. Zhou, N. Fan, M. S. Xia, L. Q. Dai, and Y. Ye, "Congo red adsorption on shell powder and chitosan-coated shell powder biosorbents: experiments and theoretical calculation," *Desalination and Water Treatment*, vol. 81, pp. 291–302, 2017.

[74] V. S. Munagapati and D. S. Kim, "Adsorption of anionic azo dye Congo red from aqueous solution by cationic modified orange peel powder," *Journal of Molecular Liquids*, vol. 220, pp. 540–548, 2016.

[75] P. N. Ikenyiri and C. P. Ukpaka, "Overview on the effect of particle size on the performance of wood based adsorbent," *Journal of Chemical Engineering and Process Technology*, vol. 7, no. 315, pp. 1–16, 2016.

[76] J. N. Wekoye, W. C. Wanyonyi, P. T. Wangila, and M. K. Tonui, "Kinetic and equilibrium studies of Congo red dye adsorption on cabbage waste powder," *Environmental Chemistry and Ecotoxicology*, vol. 2, pp. 24–31, 2020.

[77] M. I. Khan, S. Akhtar, S. Zafar et al., "Removal of Congo red from aqueous solution by anion exchange membrane (EBTAC): adsorption kinetics and themodynamics," *Materials*, vol. 8, no. 7, pp. 4147–4161, 2015.

[78] E. Rápó, L. E. Aradi, A. Szabó, K. Posta, R. Szép, and S. Tonk, "Adsorption of Remazol brilliant violet-5R textile dye from aqueous solutions by using eggshell waste biosorbent," *Scientific Reports*, vol. 10, no. 1, pp. 1–12, 2020.

[79] K. Litefti, M. S. Freire, M. Stitou, and J. González-Álvarez, "Adsorption of an anionic dye (Congo red) from aqueous solutions by pine bark," *Nature Scientific Report*, vol. 9, no. 1, pp. 1–13, 2019.

[80] T. M. Rao and V. V. B. Rao, "Biosorption of Congo red from aqueous solution by crab shell residue: a comprehensive study," *Springerplus*, vol. 5, no. 537, pp. 1–14, 2016.

[81] R. Momina, M. Rafatullah, S. Ismail, and A. Ahmad, "Optimization study for the desorption of methylene blue dye from clay based adsorbent coating," *Water*, vol. 11, no. 6, pp. 1304–1313, 2019.

[82] L. Liu, S. Fan, and Y. Li, "Removal behavior of methylene blue from aqueous solution by tea waste: kinetics, isotherms and mechanism," *International Journal of Environmental Research and Public Health*, vol. 15, no. 7, pp. 1321–1337, 2018.

[83] P. Senthil Kumar, S. Ramalingam, C. Senthamarai, M. Niranjanaa, P. Vijayalakshmi, and S. Sivanesan, "Adsorption of dye from aqueous solution by cashew nut shell: studies on equilibrium isotherm, kinetics and thermodynamics of interactions," *Desalination*, vol. 261, no. 1-2, pp. 52–60, 2010.